surements on the structure of P(H):DPPG we are not able to provide any quantitative picture of the structures formed in the solutions of P(H) and phospholipids.

(10) Demas, J. N. *Excited State Lifetime Measurements*; Academic: New York, 1983; Chapter 4.
(11) (a) Cuniberti, C.; Perico, A. *Prog. Polym. Sci.* 1984, *10*, 271. (b) Winnik, M. A. *Acc. Chem. Res.* 1985, *18*, 73.
(12) Lakowicz, J. R. *Principles of Fluorescence Spectroscopy*; Plenum: New York, 1983; Chapter 9.
(13) Arora, K. S.; Turro, N. J. *J. Polym. Sci., Polym. Chem. Ed.*, in press.
(14) This is possible in view of the low concentration of 1 (4 mg/100 mL) used in our experiments in comparison to that used by Tirrell and co-workers (1 mg/mL) in their calorimetric investigations.[1] The low concentration of 1 was required in our experiments in order to avoid interchain interactions of pyrene groups.
(15) Fendler, J. H. *Membrane Mimetic Chemistry*; Wiley: New York, 1982; Chapter 6.
(16) Mabrey, S.; Sturtevant, J. In *Methods in Membrane Biology*; Korn, E. D., Ed.; Plenum: New York, 1978; Vol. 9, p 237.
(17) Vandijck, P. W. M.; Th. Ververgaert, P. H. J.; Verkleij, A. J.; Van Deneen, L. L. M.; DeGier, J. *Biochim. Biophys. Acta* 1975, *406*, 465.
(18) Arora, K. S.; Turro, N. J., unpublished results.
(19) The required amount (4 mg/10 mL) of DPPG was hydrated at 45–50 °C in Tris buffer solution (pH 7) by ultrasonic irradiation until a clear solution was obtained. The required amount of the stock solution of P(H) or P(–) was added after the pH of the DPPG solution was adjusted to the desired value. The fluorescence spectra were recorded immediately after the pH was measured.

End-Group Effects on the Wavelength Dependence of Laser-Induced Photodegradation in Bisphenol-A Polycarbonate

J. D. Webb* and A. W. Czanderna

Solar Energy Research Institute, Golden, Colorado 80401. Received April 18, 1986

ABSTRACT: Changes in the vibrational spectra of capped and uncapped bisphenol-A polycarbonate films resulting from exposure to pulsed laser radiation at 265, 287, and 308 nm were measured quantitatively by in-situ Fourier transform infrared reflection–absorption spectroscopy. These spectra show molecular weight dependent features which indicate that phenolic end groups in the uncapped polymer, if present in concentrations exceeding the water content of the polymer, are hydrogen bonded to the backbone carbonyl groups. The correspondence of changes in molecular weight to the changes in the vibrational spectra of the exposed films was investigated by size-exclusion chromatography. These results indicate that phenolic end groups sensitize polycarbonate to some photodegradation reactions (such as cross-linking) at 287 and 265 nm, while inhibiting photo-Fries rearrangements. The hydrogen-bonded carbonyl linkages and phenolic end groups are preferentially degraded, especially at 287 nm, where phenolic end group absorption predominates. Absorption (and photoactivity) in highly (>99%) capped polycarbonate is greatly reduced at 287 nm.

Introduction

The photochemistry of bisphenol-A polycarbonate (BPA-PC) has been the subject of a number of investigations since losses of desirable properties such as transparency, tensile strength, impact resistance, and rigidity result from photodegradation when this well-known engineering polymer is used in outdoor applications.[1-3] Since many of these properties are adversely influenced by reactions at the surface of the solid polymer, where solar UV absorption and uptake of oxygen and water are highest, the addition of UV stabilizers and/or antioxidants to the bulk polymer has been generally unsuccessful in extending its outdoor service life to beyond 3 years.[4] Attempts to extend the outdoor service life of polycarbonates by incorporating them into laminates of weatherable, UV-absorbing acrylate and methacrylate polymers have also been unsuccessful, although efforts in this direction continue.[5]

The major parameters influencing outdoor photodegradation of BPA-PC include the wavelength of incident UV radiation, atmospheric oxygen and moisture, and monomer content. Wavelengths as short as 290 ± 2.5 nm may be observed on a continuous basis in the terrestrial solar spectrum,[6,7] and Barker[8] has proposed that intermittent "bursts" of solar radiation at wavelengths as short as 270 nm may penetrate to the earth's surface, based upon measurements of local diurnal variations in the effective thickness of the atmospheric ozone layer.

The first mechanistic interpretations of the photodegradation of BPA-PC were made in terms of photo-Fries rearrangements and chain scission.[9-11] More recent laboratory studies have emphasized the importance of photooxidation and cross-linking reactions in oxygen environments.[12-14] Broad-band UV irradiation or the mercury lines at 254 or 313 nm have been used to initiate photodegradation in these studies. Monochromatic light between 280 and 330 nm with a bandwidth of ±5 nm was used in a recent study of the wavelength dependence of surface photooxidation in BPA-PC.[15] The influence of residual BPA monomer on the photodegradation of BPA-PC was investigated by Pryde,[16] and the role of uncapped phenolic end groups (a processing artifact) in decreasing the thermal[17] and hydrolytic[18] stability of BPA-PC has also been described.

In this work, monochromatic laser UV radiation at 265, 272, 285, 287, and 308 ± 0.01 nm and broad-band UV radiation having various intensity distributions in the range 240–500 nm were used to investigate the wavelength dependence of photodegradation in thin films of capped and uncapped BPA-PC in dry, synthetic air. The technique of Fourier transform infrared reflection–absorption (FTIR-RA) spectroscopy was used to measure photochemically induced changes in the vibrational spectra of the BPA-PC film samples in situ. The advantages of this technique relative to others available and the optimum sample configurations have been described.[19] Changes in the molecular weight distribution of the UV-exposed films were determined by size-exclusion chromatography (SEC). Both FTIR-RA spectroscopy[20] and SEC[10,11] have been utilized to estimate the quantum yields of photoprocesses in BPA-PC.

Experimental Section

Materials and Characterization. BPA-PC polymers I–IV (Table I) were obtained from Polysciences, Inc. and were purified by precipitation from unstabilized, distilled tetrahydrofuran (THF, Burdick and Jackson) into ether or methanol. A general formula for these polymers is given in Table I. Low molecular weight,

Table I
BPA-PC Polymer Types Studied: $R_1(C_6H_4C(CH_3)_2C_6H_4OOCO)_nR_2$

BPA-PC type	R_1	R_2	% chain ends with R_1 and R_2 attached (F)	$\bar{M}_n$	av n^a	D^b	T_g, °C
I	$-OH$	$-C_6H_4C(CH_3)_2C_6H_4OH$	100	2510	8.98	1.55	111
II	$-OH$	$-C_6H_4C(CH_3)_2C_6H_4OH$	88	2850	10.3	1.88	111
III	$-OH$	$-C_6H_4C(CH_3)_2C_6H_4OH$	94	3720	13.7	2.21	117
IV	$-OOCOC_6H_5$	C_6H_5	88	18360	71.4	2.04	146
IV	$-OH$	$-C_6H_4C(CH_3)_2C_6H_4OH$	12	18360	71.4	2.04	146
V	$-OOCCH_3$	$-C_6H_4C(CH_3)_2OOCCH_3$	99	3120	11.1	1.41	113
V	$-OH$	$-C_6H_4C(CH_3)_2OH$	1	3120	11.1	1.41	113

^{a} From $\bar{M}_n$. $^b = \bar{M}_w/\bar{M}_n$.

uncapped BPA-PC polymers I–III were synthesized as described by Merrill.[21] BPA-PC IV is a commercial pelletized resin.

Acetyl-capped BPA-PC (V) was prepared by refluxing I over Mg in a 50/50 (v/v) THF/acetyl chloride (Aldrich, 98%) blend while raising the reflux temperature from 35 to 50 °C during a 4-h period, followed by precipitation into ether, filtration, redissolution in THF, filtration, and reprecipitation into methanol. The finely divided precipitate of V was dried overnight under vacuum at 100 °C. No halides were precipitated by the addition of $AgNO_3$ to a water extract of V. UV absorbance spectra of THF solutions of polymers I–V, bisphenol-A (BPA), and 4,4'-isopropylidenebis[phenyl acetate] (IPDA, prepared by dissolving BPA in acetyl chloride over Mg) were obtained with a Hewlett-Packard 8450 rapid-scanning spectrophotometer (1-nm resolution) and 1.00-cm fused-silica cuvettes. UV absorbance maxima of THF solutions of I–V were not shifted relative to those of thin solid films on quartz substrates, indicating that UV absorption coefficients obtained from THF solutions of these materials are representative of those of solid films. The absorption coefficients of I–V relative to that of BPA at 287 nm were used in conjunction with the number-average molecular weight for each polymer to determine the percentage of phenol-terminated chain ends (Table I).

Number-average molecular weights $(\bar{M}_n)$ and polydispersities (D) for I–V were calculated from SEC data of ~0.1 g/L solutions of each material in very pure THF (absorptivity at 230 nm ≤ 0.25 cm^{-1}). These data were obtained with a Varian Model 5030 HPLC system consisting of an isocratic pump operated at 1.2 mL of THF/min, high-resolution SEC columns, a Varian Model VUV-10 variable-wavelength UV detector, and a Hewlett-Packard Model 3388A integrator with SEC software. For analysis of I–III and V, an IBM 863575-3 (no. 3) SEC column, capable of resolving individual fractions of BPA-PC from monomer to $n = 8$ and linear from $M = 500$ to $M = 20\,000$ (polystyrene basis), was used. For analysis of IV, an IBM 863575-5 (no. 5) SEC column, linear from $M = 4 \times 10^3$ to $M = 4 \times 10^5$, was used. Four polystyrene (PS) primary molecular weight standards (Arro Laboratories) having M from 666 to 9000 were used to calibrate the no. 3 SEC column. Five polystyrene standards having M from 4000 to 83 000 were used to calibrate the no. 5 column. A size-correction factor[22] $(Q$ factor, $M_{BPA-PC}/M_{PS})$ of 0.72 was calculated from SEC analysis (using PS primary standards) of a polydisperse BPA-PC secondary standard (Scientific Polymer Products) having a known $\bar{M}_n$. A set of nine Q factors was obtained by dividing the molecular weights calculated with the polystyrene calibration line for each SEC-resolvable fraction (monomer to $n = 8$) of the low molecular weight polymer I into the stoichiometric molecular weight of each fraction. Averaging the results gave $\bar{Q} = 0.73 \pm 0.07$, and this value was used in subsequent determinations of $\bar{M}_n$ of BPA-PC. T_g for each material (Table I) was determined by using a Perkin-Elmer differential scanning calorimeter, Model DSC-2C, and a heating rate of 10 °C/min. The T_g data for polymers III–V exhibited the same linear dependence on inverse $\bar{M}_n$ described by Adam et al.[17] Polymers I and II exhibited positive deviations in T_g of several degrees from linearity, probably because of intermolecular hydrogen bonding of the phenolic terminal groups in these polymers.

Sample Preparation for Spectroscopic Studies. Thin-film samples of I–V were prepared on IR-reflective, gold-coated glass substrates by casting from 2.5% solutions in THF and drying in nitrogen, followed by vacuum annealing at 103 ± 1 °C for 1 h.[23]
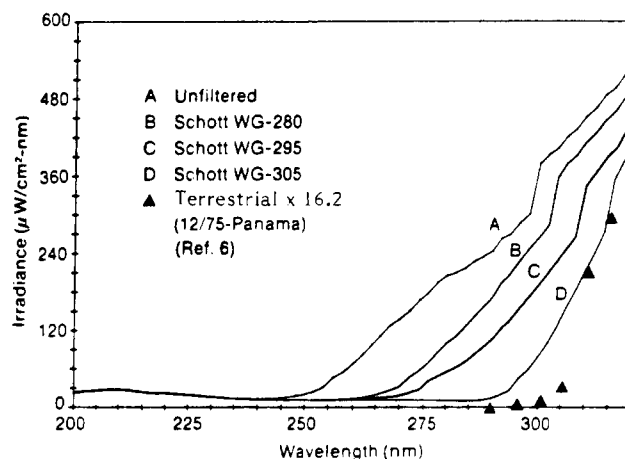

Figure 1. UV irradiance distribution produced by filtering the output of an Oriel 1000-W solar simulator compared to the terrestrial irradiance distribution calculated by assuming that the daily UV dosage[6] is received in a 1-h period near noon.

The substrates were prepared by evaporative deposition of Al and Au layers, 20 and 85 nm thick, respectively, onto $14 \times 10 \times 1$ mm float-glass slides. The resulting Au/Al/glass substrates presented a smooth, chemically inert surface for support of the cast polymer films. The thickness of the BPA-PC films was taken as the average height of six steps cut around the periphery of each annealed polymer film by solvent dissolution. The step heights were measured to a precision of ± 5 nm with a Tencor Alpha-Step surface profiler, calibrated with Sloan thickness standards traceable to NBS standards. The average thickness of the BPA-PC films varied from 67 to 210 nm. These thicknesses are within the optimum range[24] for measurement of IR-RA spectral changes in BPA-PC from 1800 to 1000 cm^{-1} and also permit the UV flux to be uniform throughout the films during exposure.

UV Sources and Calibration. A 1000-W Oriel Model 6732 solar simulator with a high-pressure, ozone-free xenon arc lamp was used as a source of broad-band UV irradiation. The simulator is equipped with a dichroic reflector (Optical Coating Laboratories, Inc.) that essentially limits the spectral output of the lamp to a band between 240 and 500 nm. Schott absorption filters were used to attenuate the short-wavelength portion of this band at 255, 260, or 287 nm. The simulator output spectra thus produced were measured at a distance from the lamp equal to that of the samples when exposed in the specular reflectance cell. The measurements (Figure 1) were made with a Gamma Scientific Model DR-2 spectroradiometer with a Si detector and single monochromator calibrated with a 1000-W tungsten source having a spectral output traceable to an NBS irradiance standard. Measurements of the simulator output spectra made with an Instruments SA Spectra-Link spectroradiometer with a Model DH-10 double monochromator, a photomultiplier tube detector, and a Melles-Griot OD-3 UV neutral-density filter confirm the earlier measurements and exhibit none of the stray light or order-sorting artifacts visible in Figure 1.

As a source of monochromatic UV radiation from 265 to 287 nm, a tuneable Lambda-Physik Model Fl-2000 dye laser utilizing Coumarin 153 dye and a potassium hydrogen phthalate crystal for frequency doubling was used. The dye laser was pumped at
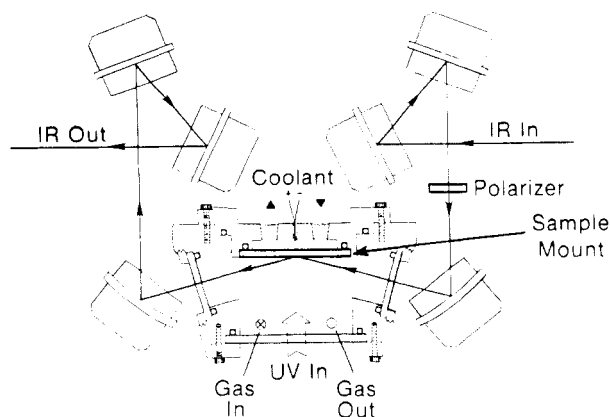
Figure 2. Specular reflectance cell enabling control of sample exposure conditions and in-situ collection of sample IR-RA spectra.

Figure 3. UV absorbance spectra of 0.04 g/L BPA and IPDA in THF solution.

308 nm by a Lambda-Physik pulsed excimer laser (Model EMG-50E) operated at 3–15 Hz and utilizing xenon chloride as the excimer species. The pulse energy of the dye laser was 50–100 μJ/pulse for 10-ns pulses, as measured before and after sample exposure with a Scientech Model 38-0105 UV calorimeter with a quartz window and thermal insulation. The wavelength accuracy of the UV dye laser was confirmed by monitoring laser power transmitted through a 290 ± 2.5 nm band-pass filter as a function of monochromator setting. During sample exposure, the output energy of the dye laser was monitored by using the reflection (approximately 10%) from a quartz beam splitter as input to a United Detector Technology UV-100 photodiode with a Schott UG-5 visible-blind filter and a Melles-Griot OD-2 UV neutral-density filter. The transient voltage output of the photoiodide was followed with an oscilloscope triggered by the excimer laser discharge circuit, and optical adjustments to the dye laser were made during sample exposure as necessary to maintain initial per-pulse energy. As an additional source of monochromatic UV radiation, the pulsed output of the excimer laser at 308 nm was also utilized by directing it with a mirror train around the dye laser and into the specular reflectance cell. The output beam area of the UV excimer laser at the end of the mirror train was 2.5 cm² (vs. 1.0 cm² for the dye laser), for 10-ns pulses at 5–7 mJ/pulse.

Sample Exposure and In-Situ FTIR-RA Spectroscopy. The polymer/gold samples were mounted in a specular reflectance cell (Figure 2), which enables in-situ measurement of the IR-RA spectra of 0.6 × 0.3 cm elliptical area at the center of each sample during exposure to UV radiation. In-plane p-polarized IR radiation was incident at a mean angle of 74° for all sample analyses, as determined by measurement of the path of the helium–neon reference laser in the FTIR spectrophotometer. Divergence of the IR beam is approximately ±3°, determined by measuring IR throughput through a series of apertures. The cell is mounted in the front IR beam path of a Nicolet 7199 FTIR spectropho-tometer with a cryogenic mercury cadmium telluride (MCT) detector. Before the sample spectra were collected, a reference spectrum of an uncoated Au reflector mounted in the cell was stored. IR-RA spectra of the samples were computed from the logarithmic ratios of the sample and reference spectra, for which 1000 interferometer scans at 2-cm⁻¹ resolution, requiring about 12 min, were used. The samples were maintained at 25–29 °C in a continuous flow of dry, CO_2-free air while being exposed to UV radiation in the cell.

Before exposure of a sample to broad-band UV radiation, the IR-RA spectrum of each sample was collected. The sample was exposed to filtered or unfiltered UV radiation from the xenon arc source for a 2-h period, during which time four additional IR-RA spectra were collected in situ. Photodegradative changes in the IR-RA spectra of the samples could be quantitatively determined by digital subtraction of the initial spectrum from those collected during exposure.

For sample exposure, laser UV wavelengths of 265, 272, 285, and 287 nm were chosen to be close to the wavelengths of UV absorbance maxima in solid BPA-PC (see Results and Discussion). Radiation at 308 nm, which is in the tail of the UV absorption edge in BPA-PC, was also utilized. Before exposure, an initial
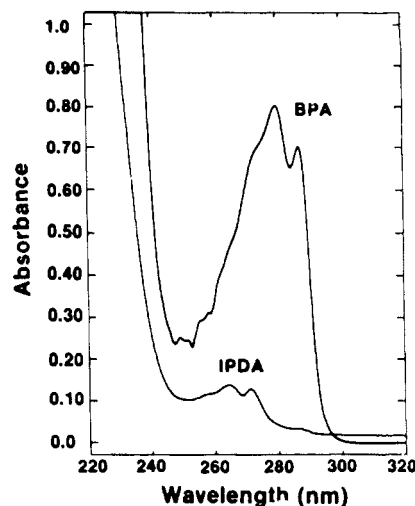
IR-RA spectrum of the sample was taken, and subsequent spectra were collected in situ after exposure of the sample to a series of laser pulses. Photodegradative changes in the IR-RA spectra were also followed by digital subtraction. This enabled the total number of laser UV pulses per sample to be limited to produce a change in the BPA-PC carbonyl band intensity (1776 cm⁻¹) of 1–10% so that only initial photodegradative changes would be measured. This criterion was met at 265 and 272 nm after 10 000 pulses, at 285 and 287 nm after 30 000–50 000 pulses, and at 308 nm after 10⁵ pulses. Several IR-RA spectra were taken of each sample after intermediate numbers of laser pulses to determine the linearity of IR-RA spectral changes with UV exposure.

SEC Analysis of Exposed Samples. After UV exposure, the supported polymer film samples were removed from the cell and their thickness was remeasured. The exposed area of the polymer films (about 1 cm²) was dissolved in about 0.2 mL of THF by dropping the solvent onto the sample surface and drawing the resulting polymer solution, containing about 10 μg of BPA-PC, back into the syringe. This process was repeated until most of the exposed polymer was dissolved. The samples were then injected into the appropriate SEC column for determining their molecular weight and their molecular weight distributions (MWD). Polystyrene primary standards and BPA-PC secondary standards (for IV) were injected before and after each set of three or four samples to factor any variations in column elution rate into the time-based MWD calculations. Flow variations were minimal or negligible.

Results and Discussion

UV Absorbance Spectra of BPA-PC (I–V), IPDA, and BPA. The UV spectra of commercial BPA-PC (IV) in tetrahydrofuran (THF) solution and as a thin solid film on quartz sheets show the edge of a weak system of bands at 290 nm and a stronger band edge at 240 nm. Maxima are distinguishable in these spectra at 286, 271, 264, and 230 nm. In dichloromethane, the absorbance maximum of the weak band at 286 nm is shifted to 283 nm; wavelengths of the other UV absorbance maxima are un-changed.

The influence of phenolic end groups in shifting the UV absorbance maxima of BPA-PC at 264 and 271 nm to longer wavelengths, as well as increasing its UV absorption coefficients, may be inferred from a comparison of the UV absorbance spectra (Figure 3) of BPA monomer and its acetylated derivative, IPDA. IPDA is a monomeric ana-logue of a BPA-PC repeating unit and exhibits absorption maxima at 264 and 271 nm, as does BPA-PC, with ab-sorption coefficients close to those of IV and V at these wavelengths. In BPA, these bands are shifted by 15 nm to 279 and 286 nm, with BPA exhibiting a seven-fold in-
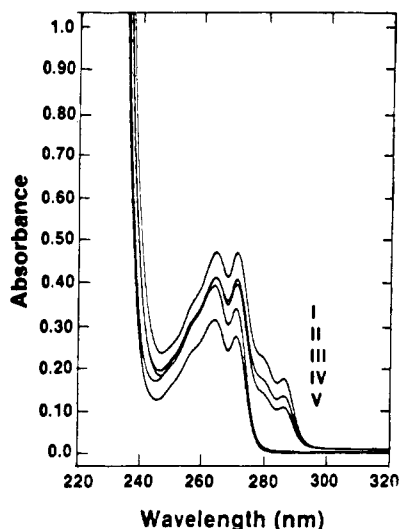
Figure 4. UV absorbance spectra, normalized to 0.100 g/L, of BPA-PC polymers I–V in THF solution.
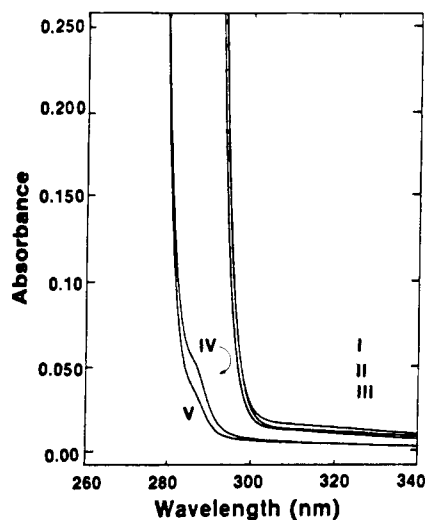

Figure 6. UV absorbance spectra, normalized to 2.00 g/L, of BPA-PC polymers IV and acetylated IV in THF solution.

Figure 5. UV absorbance spectra of ∼2 g/L BPA-PC polymers I–V in THF solution.

Figure 7. Size-exclusion chromatographs of BPA-PC polymers I–V (before exposure) and of a BPA-PC multidisperse secondary molecular weight standard ($\bar{M}_n = 14\,400$, $D = 2.65$). Plot markers indicate elution times, 3.5–7 min.

crease in its absorption coefficients at these wavelengths relative to those of IPDA (and BPA-PC repeating unit) at 264 and 271 nm. This wavelength shift is very noticeable in the UV spectra of I–III (Figure 4) and can be distinguished in the UV spectrum of IV, which has about twice the concentration of phenolic end groups as V. The UV spectra of more concentrated solutions of I–V (Figure 5) show the long-wavelength shift of IV relative to V more plainly and reveal that "tailing" absorption extends to at least 400 nm, which therefore greatly increases absorption of terrestrial solar radiation[6-8] by I–IV. The tailing absorption results from either phenolic end groups or oxygen charge-transfer complexes[12] associated with phenolic end groups. Figure 6 shows that the tailing UV absorption and the relatively high content of phenolic end groups[17] in commercial BPA-PC (IV) may be reduced by aceylation under conditions similar to those used to produce V from I. There is some evidence that the phenolic end group content of the as-received commercial polymer is higher than that measured immediately after production,[25] perhaps because of slow oxidation or hydrolysis[18] upon extended storage.

Size-Exclusion Chromatography (SEC) of I–V and BPA. Size-exclusion chromatographs of I–V (before exposure) and of a BPA-PC secondary standard ($\bar{M}_n =$
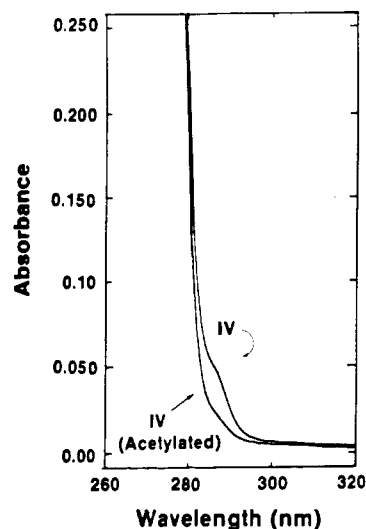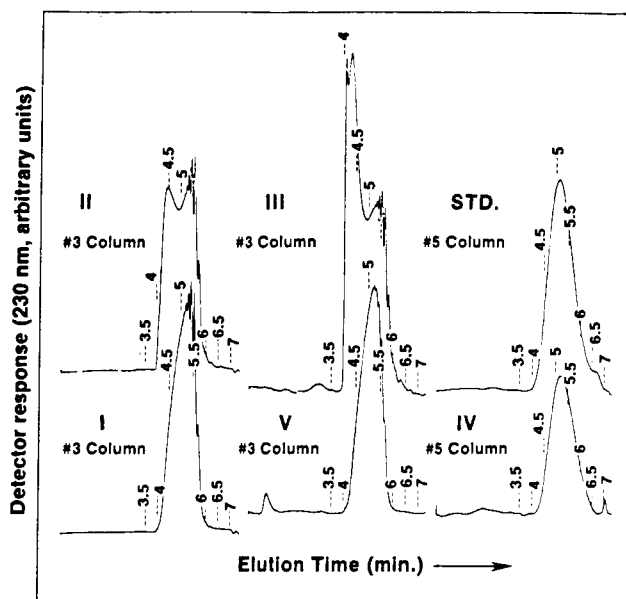
14 000, $D = 2.65$) are reproduced in Figure 7. In the chromatographs of I–III, fractions from monomer (6.6–6.7 min) to $n = 8$ are present and clearly resolved by the no. 3 column. The elution time of BPA monomer was confirmed by SEC analysis of a blend of I and BPA. In the chromatograph of V, only the trimer (5.7 min) to $n = 8$ fractions were visible. For SEC of IV and the BPA-PC secondary standard, the no. 5 SEC column was used instead of the no. 3 column and individual fractions of these high molecular weight polymers were not resolved. Analysis of IV with the no. 3 column indicated that no chains having $n = 8$ or fewer repeating units were present prior to exposure. The peak at 7.1 min in the chromatograph of IV and that at 0.8 min in the chromatograph of V (Figure 7) are artifacts produced by the packing in the sample injection valve and did not interfere with the molecular weight calculations. The bimodal appearance of the chromatographs of II and III apparently resulted from exceeding the exclusion limit of the no. 3 column. Therefore, the data for initial $\bar{M}_n$, $\bar{n}$, and F (Table I) for II and III may be low by 6–12% on the basis of UV end-

Table II
Gaussian k_2 Parameters for Quantitative Analysis of BPA-PC Polymers I–V and Photoproducts

ν_0, cm^{-1}	$k_2(0)^a$	σ, cm^{-1}	$n_2\infty$	structural assignment^b
1776	0.24	10.0	1.41	main-chain carbonyl
1768	0.20	4.5	1.41	terminal acetyl carbonyl (V)
1750	0.24^c	10.3	1.41	H-bonded carbonyl
1685	0.30	10.0	1.41	main-chain salicylate
1644	0.22	5.0	1.41	terminal o-hydroxy ketone (V)
1515	0.24	3.5	1.38	terminal 4-phenol or BPA
1507	0.19	7.0	1.38	main-chain aromatic
1485	0.01	7.0	1.38	substituted aromatic
1247	0.50	23.0	1.45	C–O (I, II, III) + C=O
1235	0.68	16.0	1.45	C–O (IV, V) + C=O
1225	0.22	9.0	1.45	C–O (I, II, III) + C=O
1194	0.55	8.5	1.45	C–O (I, II, III) + C=O
1194	0.62	7.0	1.45	C–O (IV, V) + C=O
1164	0.46	5.0	1.45	C–O + C=O

^{a} Calculated for a mole fraction of unity vs. repeating units in a solid polymer of infinite chain length. ^{b} I–V unless otherwise noted. ^{c} Assumed to equal $k_2(0)$ at 1776 cm^{-1}.

group analysis. The effect of this error upon calculation of *changes* in $\bar{M}_n$ for these polymers was negligible.

Optical Constants and Absorbance Band Assignments in I–V and Photoproducts. To derive quantitative measurements of changes in the covalent bond structure of the polymer films from measurements of changes in their IR-RA spectra, it is necessary to simulate these spectra with an appropriate optical model. The Fresnel equations for each sample can be solved[24] to predict IR-RA at the fundamental vibrational frequencies (ν_0) if the spectral IR optical constants of the polymer films ($N_2(\nu) = n_2 - ik_2$) and the metallic substrates ($N_3(\nu) = n_3 - ik_3$) as well as the average polymer film thickness (d) and mean incidence angle (θ) of the IR radiation in the reflectance cell are accurately known. Both d and θ were measured as described in the previous section. The real and complex coefficients, n_3 and k_3, of the spectral optical constants [$N_3(\nu)$] of the substrates are available.[26] The spectral IR optical constants [$N_2(\nu)$] of IV, computed at 2-cm^{-1} resolution from the polarized surface reflectance spectra of a 3-mm-thick sheet of the polymer,[20,24] were utilized as a basis for calculation of the IR optical constants of I, II, III, and V. Because of noise in the measured k_2 spectrum of IV, an indirect procedure was used to derive a Gaussian fit to the k_2 spectrum. This procedure involved fitting the measured n_2 spectrum of IV with a simulated n_2 spectrum derived from numerical Kramers–Kronig integration[24] of an additive series of Gaussian (normal) k_2 distributions defined by eq 1, where σ is the standard

$$k_2(\nu) = k_2(\nu_0)\ \exp\{-\tfrac{1}{2}[(\nu - \nu_0)/\sigma]^2\} \qquad (1)$$

deviation of the distribution. With this procedure, it was found that the fundamental frequencies of strong absorbances observed in samples of undegraded IV to which definite structural assignments may be made (Table II) are 1776, 1507, 1235, 1194, and 1164 cm^{-1}. Other absorbances in the undegraded polymer either are so weak that changes in their IR-RA spectra cannot be measured concurrently with changes in the strong absorbances in the samples analyzed, as predicted previously,[24] or these absorbances have not been assigned to specific structures. The absorbance at 1164 cm^{-1} has been assigned to a carbon–carbon vibration;[11] however, the absence of this band in the spectrum of 2,2-diphenylpropane and its presence in the spectra of many aromatic ethers and esters[27] indicates that this band is a C–O vibration. Structural assignments for the other strong absorbances in IV are consistent with the available literature.[11,16,27,28] The lack
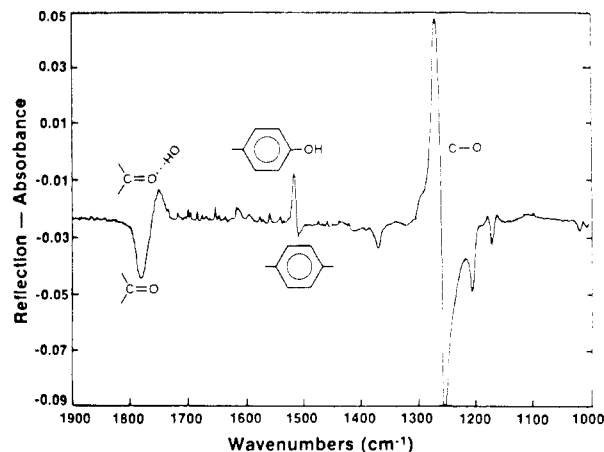

Figure 8. Subtraction spectrum generated between IR-RA spectrum of uncapped BPA-PC (I) and IR-RA spectrum of acetyl-capped BPA-PC (V) times a thickness correction factor of 1.18.

of a distinguishable carbonyl absorbance at 1768 cm^{-1} in I–IV indicates that the BPA-PC films are completely amorphous.[28]

Increases in absorbance at 1685 cm^{-1} in BPA-PC have been ascribed[11] to the first step of photo-Fries rearrangement of the carbonate backbone. The absorptivity coefficient k_2 for the product of this reaction was estimated[29] by using $k = 2.303\epsilon C/4\pi\nu$ and the molar absorptivity ϵ at $\nu = 1685$ cm^{-1} of phenyl salicylate in THF solution. The standard deviation (σ) was estimated from the half-width of the absorbance band at two-thirds maximum intensity. The concentration C of repeating units in solid IV is 4.72 M.

The second step of the photo-Fries rearrangement is also possible in BPA-PC.[10,11] The IR spectra of 2,2'-dihydroxybenzophenone solutions in THF show a carbonyl absorption at 1690 cm^{-1} with a molar absorptivity about 10 times less than that of phenyl salicylate at 1685 cm^{-1} and reveal no other features by which the two compounds (analogues to photo-Fries product in BPA-PC) can be distinguished. Although most spectral changes in I–V at 1685 cm^{-1} are therefore expected to result from accumulation of strongly absorbing, salicylate-like groups, a contribution from the second product of photo-Fries rearrangement cannot be ruled out. No absorbance at 1685 cm^{-1} was detected in I–V before exposure.

The absorbances at 1610, 1590, and 1485 cm^{-1} are related to the number and polarity of substituents to the BPA-PC aromatic rings and are more intense in the spectra of photo-Fries rearrangement products. However, other reactions such as photooxidation[12] can produce increased ring substitution in BPA-PC, and therefore, these absorbance bands are not quantitatively useful. The band at 1485 cm^{-1} was included in Table II because it partially overlaps the quantitatively useful band at 1507 cm^{-1}.

The slight differences in the vibrational spectra of capped and uncapped BPA-PC containing phenolic chain ends are revealed by digital subtraction of the IR-RA spectrum of I from that of V times a thickness correction factor. The resulting subtraction spectrum (Figure 8) shows positive absorbances at 1750, 1610, 1590, and 1515 cm^{-1} and negative absorbances at 1776, 1507, and 1370 cm^{-1}. The positive absorbance at 1515 cm^{-1} is due to terminal phenolic groups in I and corresponds to the aromatic C=C stretching vibration in BPA. The Gaussian parameters for the band (Table II) were estimated from the IR spectrum of BPA in THF by using $k = 2.303\epsilon C/4\pi\nu$. The positive absorbance at 1750 cm^{-1} is due to main-chain carbonyl groups in I, which are either inter- or intramo-

lecularly hydrogen bonded to the terminal phenolic hydrogen or to other polar molecules such as BPA and H_2O, as proposed by Farenholtz[30] and Pryde.[16]

The absorbance at 1768 cm⁻¹, due to the terminal acetyl carbonyl in V, can be observed more distinctly than in Figure 8 by subtracting the IR-RA spectrum of IV from that of V. The Gaussian k_2 parameters for this band (Table II) were derived from analysis of the IR absorbance spectrum of phenyl acetate in THF. Some samples of V exhibited an increase in absorbance at 1644 cm⁻¹ after UV exposure, apparently due to Fries-like rearrangement of the terminal phenyl acetyl carbonyl to give an o-hydroxyacetophenone, which exhibits a carbonyl absorption maximum at this frequency.[27] The Gaussian k_2 parameters for this band (Table II) were derived from the spectrum of o-hydroxyacetophenone in THF.

The subtraction spectrum (Figure 8) also exhibits considerable differences in IR-RA between samples I and V in the C–O bonding region from 1300 to 1000 cm⁻¹, with the exception of the band at 1164 cm⁻¹. Since nonlinear optical effects prevail in this region,[24] subtraction spectra cannot be easily interpreted within it, and most of the ester absorption bands of dissolved BPA-PC are masked by solvent absorption. To obtain the Gaussian k_2 parameters for I, II, and III in this region without resorting to a polarimetric technique,[24] the absorbance spectrum of II dispersed at 10^{-4} weight fraction in KBr was fit with a combination of Gaussian distributions (eq 1) using a curve-fitting algorithm, CAP, which is part of the Nicolet 7199B software package. In this procedure, the absorbance band at 1164 cm⁻¹ served as a reference for calculation of the values of k_2 at 1247, 1225, and 1194 cm⁻¹ (Table II) for I–III. The absorption spectrum of V in this region is close enough to that of IV to enable use of the optical constants of IV to simulate the IR-RA spectra of V. The absorbance band at 1235 cm⁻¹ in solid IV is shifted to 1247 cm⁻¹ in chloroform and to 1228 cm⁻¹ in THF. Solvent absorption obscured the other ester bands. Similar solvent shifts are observed[28] in the carbonyl band at 1776 cm⁻¹, indicating that the C–O and carbonyl vibrations are coupled in the carbonate ester. The IR absorbance maxima of IV in THF solution are closer in frequency to those of the solid polymer than those observed in chloroform solutions, as were the UV absorbance maxima of I–V, indicating that optical constants calculated from THF solutions of these polymers will better approximate those of the solid polymers. The measured optical constants for IV closely resemble those measured for BPA-PC films by Ribbegard and Jones.[31]

The absorbance at 1750 cm⁻¹ is clearly visible (Figure 9) in the IR-RA spectra of I–III and is much weaker in the spectra of IV and V. If the value of k_2 for the hydrogen-bonded carbonyl at 1750 cm⁻¹ equals that of the free carbonyl at 1776 cm⁻¹, the ratio of hydrogen-bonded carbonyl groups to phenolic end groups in samples I–III is 0.70 ± 0.02. In an unannealed sample of I, this ratio is only 0.50 but rises to 0.70 after annealing for 1 h at 102 °C under vacuum. That not all of the available phenolic end groups are hydrogen bonded to carbonyl groups is also consistent with earlier studies of BPA-PC.[30] The strong molecular weight dependence of the hydrogen-bonded carbonyl absorption in I–III (Figure 9) indicates that most of this absorption results from bonding between terminal phenols and main-chain carbonyl groups. In contrast, the absorption at 1750 cm⁻¹ in IV and V, which is more intense than that predicted with an optical model[24] for the edge of the free carbonyl band centered at 1776 cm⁻¹, is greater than the absorbance expected if all of the available phe-
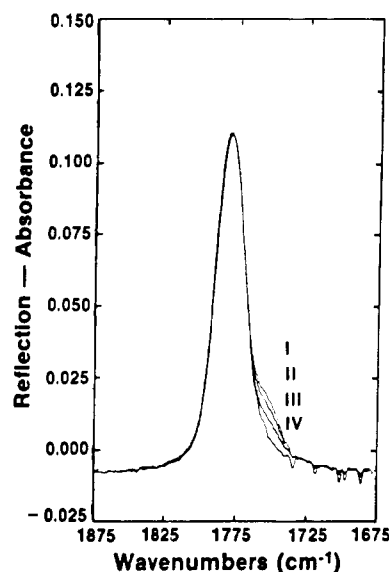

Figure 9. IR-RA spectra of BPA-PC polymers I, II, III, and V showing absorbance of free (1776 cm⁻¹) and hydrogen-bonded (1750 cm⁻¹) carbonyl groups (before exposure) normalized at 1776 cm⁻¹.

nolic end groups were hydrogen bonded to carbonyl groups. This indicates that more carbonyl groups in IV and V are hydrogen bonded to water or other small, polar molecules than to phenolic end groups, although the overall fraction of hydrogen-bonded carbonyl to free carbonyl in IV and V is only a few percent. The hydrogen-bonded carbonyl groups may form the periphery of the "polar clusters", containing phenolic end groups and small polar molecules, in the model proposed by Pryde.[18]

Quantitative IR-RA Spectroscopy of I–V. To determine quantum yields of the various photoreactions observable with IR-RA spectroscopy, it is necessary to calculate the number of chemical bonds broken or created per sample during exposure. In the following theoretical treatment, the fundamental frequencies for each functional group rather than frequencies of IR-RA band maxima, which are often higher,[29] will be utilized. For an isolated IR-RA band in a sample that is optically thin throughout the experiment at the fundamental frequency of the absorbing group, the change in IR-RA at that frequency is linear with respect to change in concentration of the absorbing species.[24] For the samples studied, these conditions are strictly met only by the IR-RA bands at 1685 and 1644 cm⁻¹, corresponding to the products of photo-Fries rearrangement. The carbonyl and aromatic bands (1776, 1768, and 1507 cm⁻¹) overlap with photoproduct bands at 1750 and 1485 cm⁻¹, and the C–O ester bands from 1247 to 1164 cm⁻¹ overlap with each other and also are not linear with changes in k_2 even in the thinnest polymer films studied.[24]

To address these problems, the single-frequency optical model[24] was enhanced to permit calculation of changes in k_2 from changes in IR-RA at the fundamental frequencies of up to ten different functional groups, which may exhibit nonlinear, overlapping IR-RA bands. This was accomplished by noting that the n spectrum of the polymer can be derived by a numerical Kramers–Kronig integration of a linear combination of Gaussian k_2 distributions (eq 1) if $n_2\infty$ is known.[24] Thus, the IR-RA of a polymer over a given wavelength interval can be determined as a function of k_2 alone if the parameters describing the Gaussian k_2 distributions within that interval are known. A computer program (DELRI) was developed that accepts these parameters and determines the value of n_2 at each fundamental vibrational frequency of interest and then determines IR-
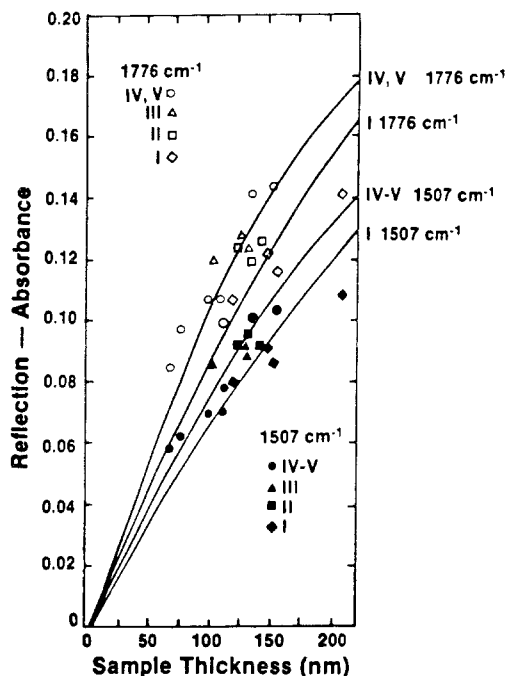
Figure 10. Predicted and measured IR-RA at 74° incidence angle wi..i p-polarization for carbonyl and aromatic absorptions in I–V as a function of film thickness; predicted IR-RA curves for II and III (not shown) are between those of I and IV, V.

RA at that frequency, providing that the polymer film thickness, substrate optical constants, and IR incidence angle and ellipticity are given. Estimates of IR-RA made in this fashion were generally within ±15% of measured values (Figure 10), with a few larger deviations apparently caused by error in the sample thickness measurements. Input of the measured IR-RA after sample exposure as a fraction of initial IR-RA eliminates the need for an exact prediction of IR-RA for each sample by the software. An initial estimate of k_{2j} for $j = 1$ to m adjacent bands is made after sample exposure by multiplying the initial values of k_{2j} by the fractional RA_j at each fundamental frequency and predicting a new set of RA_j. If the values of RA_j are linear with respect to k_{2j}, the new predictions will equal the measured fractional RA_j. If the difference between the predicted and measured RA_j exceeds a preset tolerance, a search for the set of k_{2j} values satisfying the measured RA_j (initial $RA_j + \Delta RA_j$) is begun by numerically evaluating the matrix of partial differentials

$$\sum_j \frac{\partial RA_i}{\partial k_{2j}} \Delta k_{2j} = \Delta RA_i \qquad (2)$$

for $i, j = 1$ to m. The computed changes in k_{2j} (Δk_{2j}) are added to the initial k_2 values, new n_{2j} are calculated, and a new set of RA_j is computed. If the tolerance is not met, the process is repeated. For BPA-PC C–O ester bands ($m = 3$ or 4) and fractional RA changes of <10%, convergence usually is achieved after one or two iterations. The DELRI algorithm has some resemblance to those used by Ribbegard and Jones[31] and Graf et al.[32] to calculate optical constants of free-standing polymer films. The estimates for changes in k_{2j} based on measured changes in RA_j are sensitive to the set of Guassian parameters describing the k_{2j}. For this reason, the accuracy of the predictions of initial IR-RA (Figure 10) based on these parameters and $n_3 = 2.13$ and $k_3 = 41.7$ for gold[26] is encouraging, although exact predictions are not necessary. The DELRI software is available from the authors.

'JV-Induced IR-RA Spectral Changes in Films of . The series of IR-RA spectra in Figure 11 illustrate
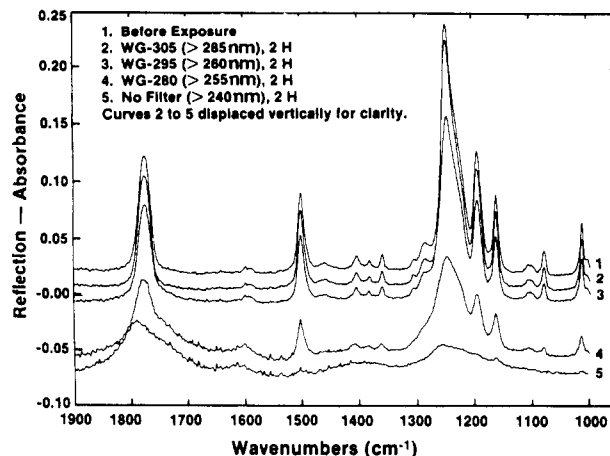

Figure 11. Cumulative effect of exposure to broad-band UV radiation at successively shorter wavelengths on the IR-RA spectrum of IV.

the dramatic influence of irradiation wavelength upon rates and mechanisms of photodegradation reactions in BPA-PC, as well as the spectroscopic advantages of using optically thin polymer films. Exposure in a synthetic air atmosphere at 25 °C to broad-band UV radiation at wavelengths greater than 287 nm (Figure 1) for 2 h produces only small changes in the IR-RA spectrum of an 88-nm-thick film of IV on gold (compare curves 1 and 2, Figure 11). Successive exposures of the same sample to UV radiation at shorter wavelengths produce substantially greater cumulative effects, most noticeably a reduction in intensity of all of the prominent IR-RA bands. In earlier studies of optically thick films,[19] only reductions in intensity of weak IR-RA bands could be observed. After an 8-h exposure sequence including a 2-h exposure to the unfiltered output of the xenon arc lamp ($\lambda > 240$ nm), the BPA-PC carbonyl absorption is the most prominent feature remaining in the IR-RA spectrum, although the band has broadened and shifted to higher frequencies. The value of k_2 for the BPA-PC carbonyl band is low enough to be essentially linear with carbonyl bulk concentration in samples thinner than 1 μm,[24] so the broadening and shifting of this band are unlikely to be optical artifacts. Oxidative formation of aliphatic anhydrides, as suggested by Factor and Chu,[12] would account for the persistence of the carbonyl IR-RA band relative to those characteristics of C–O (1164–1247 cm^{-1}) and the broadening and up-shifting of the carbonyl band. Upon removal of the sample from the specular reflectance cell, it was observed that the originally transparent film had become orange. The thickness of the film had decreased from 88 to 26 nm during the exposure sequence, and the orange residue was found to be insoluble in THF, an indication that extensive cross-linking had taken place. Chain fragmentation to produce volatile H_2O, CO, CO_2, acids (including formic and acetic), conjugated ketones, and phenols, which has been demonstrated by Factor and Chu[12] for irradiation of BPA-PC with $\lambda > 280$ nm, would account for the observed reduction in film thickness and the almost total disappearance of aromatic IR-RA (1507 cm^{-1}). Photoablation of polymer films as a result of exposure to UV radiation is well enough established to have industrial applications;[33] therefore, its observation in these studies is not surprising.

The photodegradation induced in the latter sample was so extensive that quantitative analysis of the IR-RA spectral changes could only be performed on spectra obtained early in the experiment, and SEC of the exposed sample could not be performed at all because of the insolubility of the residual polymer film. To avoid these
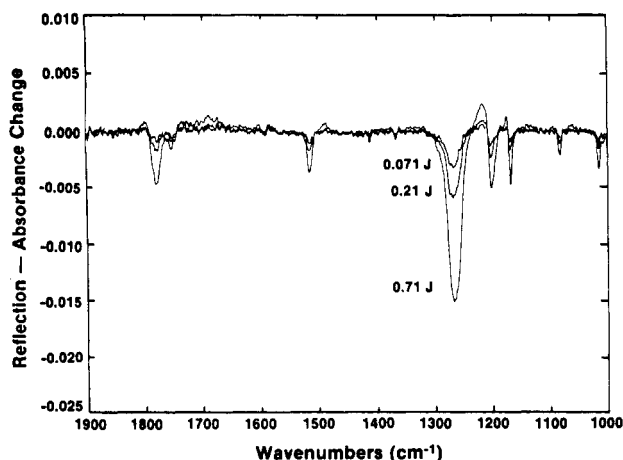
Figure 12. Subtraction spectra generated between IR-RA spectra of I collected before and after exposure to 10^3, 3×10^3, and 10^4 laser pulses at 265 nm.
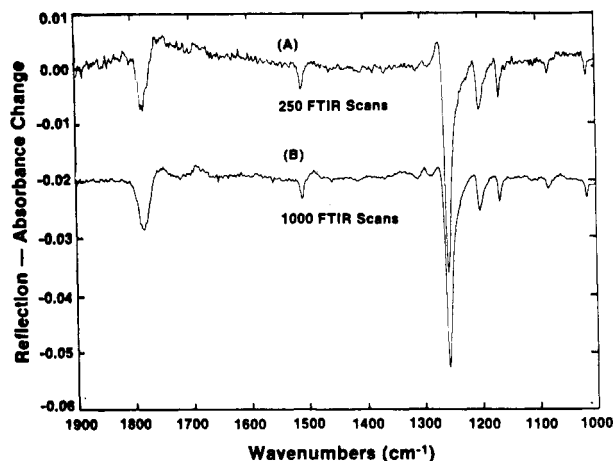
Figure 13. IR-RA spectral changes in IV resulting from exposure to 260–500-nm radiation (A) and to 10^4 laser pulses at 272 nm (B).

Figure 14. IR-RA spectral changes in I resulting from exposure to pulsed UV laser radiation at different wavelengths and total energies.

problems, the laser-exposed samples were given only enough UV laser pulses to induce changes in their IR-RA band intensities sufficient for quantitative analysis (1–10%). The relative changes in k_2 for the polymer and photoproduct absorption bands, as determined from the IR-RA spectral changes (Figure 12) for each sample using the DELRI algorithm (eq 1 and 2), were linear with UV dosage, although the IR-RA changes generally were not. This linearity indicates that competitive absorption and/or quenching by photoproducts[11,34] was not important in the thin BPA-PC films during the limited exposure sequences utilized. Figure 12 also exemplifies the high signal-to-noise ratios and good base line stability obtained with the in situ IR-RA technique.

The possibility of second-order (multiphoton) photochemistry in polymer samples exposed to intense UV radiation has been considered.[7,34] Figure 13 compares IR-RA spectral changes of a sample of IV (Figure 10) exposed to radiation from 260 to 500 nm (WG-295 filter, Figure 1) for 1 h to those of another sample exposed to 10 000 laser pulses at 272 nm, resulting in absorption of about twice as many UV quanta. It can be seen that the qualitative features of the subtraction spectra are almost identical, indicating that the photochemical reaction mechanisms in the two samples are similar (the upper spectrum is noisier because only 250 FTIR scans were utilized to generate the two parent spectra). It is also clear that the quantum yields of photodegradation processes in the sample exposed to broad-band UV were only about twice
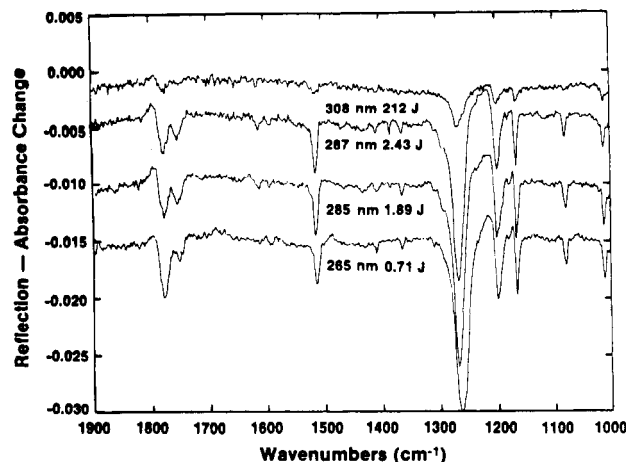
those in the sample exposed to laser radiation at 272 nm, despite the fact that the rate of photon uptake in the laser-exposed sample was 8 orders of magnitude higher than that in the sample exposed to broad-band UV. The similarity between photodegradation reaction mechanisms and quantum yields in the two samples indicates that nonlinear (multiphoton) processes did not contribute to photodegradation of the laser-exposed samples. This conclusion is not surprising when it is considered that even at the highest rate of photon uptake, only 1 in every 3000 repeating units in the laser-exposed samples, or only 1 in every 40 molecules of IV, absorbed a quantum during each laser pulse. Also, the lifetimes of excited states in BPA-PC[34] are much shorter than the interval between laser pulses ($\sim$0.1 s).

A better explanation of the relatively small differences between the efficiency of photodegradation measured in UV laser-exposed samples and in samples exposed to broad-band UV is in terms of wavelength-dependent photochemistry. The wavelength dependence of photoprocesses in I is shown in Figure 14. A relatively large input of laser energy at 308 nm is required to induce measurable changes in the IR-RA spectrum of I because of its low UV absorbance at this wavelength (Figure 4). It is also apparent from Figure 14 that at shorter laser wavelengths, much less energy is required to induce measurable IR-RA changes in the exposed samples of I. At 285 and 287 nm, where absorption by phenolic end groups in I predominates (Figures 3 and 4), a higher proportion of hydrogen-bonded carbonyl (1750 cm^{-1}) is lost relative to free carbonyl (1776 cm^{-1}) than at 265 or 308 nm. This indicates that those BPA-PC carbonyl groups which are hydrogen bonded to terminal phenols are preferentially degraded at the wavelengths of preferential UV absorption by terminal phenols. In support of this conclusion, the narrowness of the IR-RA differential band characteristic of loss of aromatic structure (1515–1507 cm^{-1}) in the samples exposed at 285 and 287 nm (Figure 14) indicates that more terminal phenolic groups (1515 cm^{-1}, $\sigma = 3.5$ cm^{-1}) are degraded at these wavelengths than at 265 nm, where loss of backbone aromatic groups (1507 cm^{-1}, $\sigma = 7$ cm^{-1}) is more significant. The absence of detectable photo-Fries rearrangement products (1685 cm^{-1}) or increases in aromatic substitution (1485 cm^{-1}) at wavelengths longer than 265 nm in I is also noticeable in Figure 14.

Repetition of these experiments with samples of II–V provided further evidence for the influence of phenolic end groups on the photodegradation of BPA-PC. Figure 15
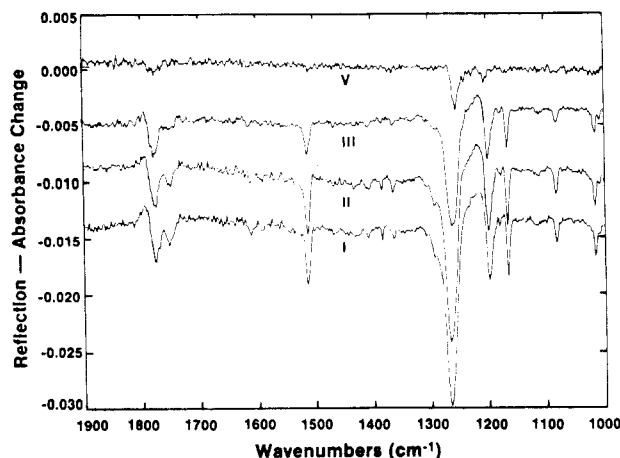
Figure 15. IR-RA spectral changes in I, II, III, and V resulting from exposure to pulsed UV laser radiation at 287 nm. The spectra are normalized to 2.08 J total UV dosage and a polymer film thickness of 103 nm.

Figure 16. Fractional UV absorptance of BPA-PC film (I) on gold as a function of film thickness/wavelength (d/λ).

shows the influence of the concentration of phenolic end groups, which increases in the order V, III, II, and I, upon the rate and mechanism of photodegradation in BPA-PC at 287 nm. The extent of IR-RA spectral changes in I, II, and III decreases in the order of end-group concentration (Table I), and V exhibits only small changes in its IR-RA spectrum for the same energy dosage at 287 nm. In the synthesis of V, most of the phenolic end groups in I were capped with acetyl groups, greatly reducing the absorption at 287 nm. As the concentration of phenolic end groups increases, the extent of degradation of hydrogen-bonded carbonyl groups (1750 cm^{-1}) increases relative to that of free carbonyl (1776 cm^{-1}). Evidence for the depletion of main-chain aromatic groups is visible at 1507 cm^{-1} for V and III but is not apparent in I and II, where depletion of terminal aromatic groups (1515 cm^{-1}) predominates. The increase in C–O absorption at 1225 cm^{-1} in I–III and the difference in frequency between the other C–O bands of I–III and those of V can also be gleaned from Figure 15. The lack of an absorption increase at 1685 cm^{-1} in V and I–III following exposure at 287 nm indicates that photo-Fries 1 or 2 are not important photoproducts at this wavelength, although subtraction spectra of IV (not shown) indicate that a slight increase in absorption at 1685 cm^{-1} occurs following exposure of IV at 287 nm.

Quantum Yields of Photodegradation in I–V. To simplify interpretation of the large quantity of spectroscopic and chromatographic data collected on exposed samples of I–V and to correct for the differences in sample thickness, exposure wavelength, and UV absorption, these data were interpreted in terms of quantum yields. For the purposes of this study, quantum yields are defined as the number of covalent bonds broken or formed as a result of exposure divided by the total number of quanta absorbed during exposure, using a 1-cm^2 area of exposed sample as a basis. Since the number of quanta absorbed by each sample could not be measured but was estimated from the UV absorption coefficients measured for solutions of I–V at the exposure wavelengths, the calculated quantum yields should be considered as *estimates* useful primarily for comparative purposes. However, the linearity of changes in k_2 with radiation dosage in the exposed samples indicates that the UV absorption coefficients of the polymer ground state did not change significantly during the experiments. To estimate the fraction of incident UV radiation absorbed by the samples, the thin-film optical model[24] was modified to calculate the absorptance (frac-
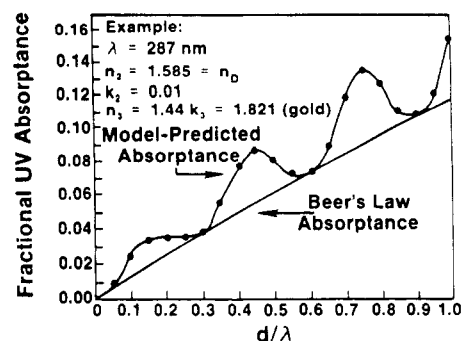
tional UV absorption, in contrast to absorbance, which is the negative logarithm of transmittance) of the BPA-PC films on gold substrates at normal incidence. For this estimate, the UV optical constants of gold,[35] $n_D = 1.585$ for BPA-PC,[36] and the measured thicknesses of the BPA-PC films and gold substrates were utilized. The value of k_2 for each polymer film at its exposure wavelength was calculated by using $k = 2.303\epsilon C/4\pi\nu$ from the measured UV absorption coefficients.

Figure 16 shows a typical set of absorptances calculated for various thicknesses of I. Because of reflection and interference effects, the absorptances calculated with the optical model for the BPA-PC films on gold substrates are equal to or greater than the estimates made with Beer's law, neglecting reflection and interference, for free-standing films of I of similar thicknesses in air. The model-calculated absorptances were used in conjunction with the energy dosage measured during exposure of each sample to estimate the total number of quanta absorbed by each sample.

To calculate the number of covalent bonds broken or formed in a volume of polymer film defined by a 1-cm^2 exposed area and the measured film thickness, the relative changes $\Delta k_2/k_2(0)$ for the sample were calculated with the DELRI algorithm (eq 1 and 2). The initial k_{2j} values for each polymer type were calculated by using $k_{2j}(0) = X_j k_{2j}$ from the limiting k_2 values in Table II and the mole fractions X_j for the corresponding functional group calculated from the data in Table I.

For example, the $k_{2j}(0)$ values for IV at 1507 and 1515 cm^{-1} are 0.1897 ($j = 1$) and 0.0004 ($j = 2$), while those for I are 0.1710 and 0.0240, respectively. For IV and V at 1750 cm^{-1}, X_j was calculated from the ratio IR-RA(0)$_{1750}$/IR-RA(0)$_{1776}$ since IR-RA$_{1750}$ was greater than that predicted from the concentration of phenolic end groups (Table I) in IV and V.

The bands in the 1776–1750-, 1515–1485-, and 1247–1164-cm^{-1} ranges were grouped together for analysis (eq 1 and 2) since the IR-RA bands within these ranges overlap each other but are sufficiently isolated from other IR-RA bands to be considered independently of them. The bands at 1685 and 1644 cm^{-1} are independent of other IR-RA bands; therefore, the DELRI algorithm was not necessary in their case. The relative changes in k_2 of these carbonyl bands were calculated by using $\Delta k_2/k_2(0) = (\Delta\text{IR-RA}_\nu/$ IR-RA(0)$_{1776})(0.24/k_2(0)\nu)$, where the $k_2(0)_\nu$ values used were taken from Table II and $\nu = 1685$ or 1644 cm^{-1}.

To determine the number of covalent bonds broken or formed in the sample volume, $10^{-7}d$ cm^3, from the relative changes in k_2 for each sample, eq 3 was used, where $C =$

$$D_j = mdCX_j\Delta k_{2j}/k_{2j}(0) \qquad (3)$$

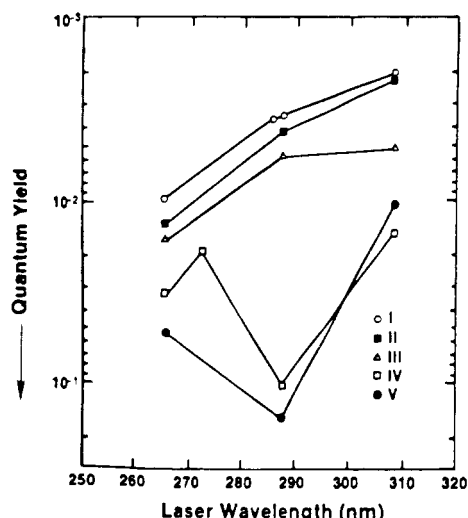2.85×10^{14} is the number of repeating units for a 1 cm^2

Figure 17. Quantum yields of free carbonyl bond depletion (1776 cm^{-1}) in BPA-PC (I–V) at several laser irradiation wavelengths. Error is ±4%.

× 1 nm volume of BPA-PC of infinite chain length and density of 1.20 g/cm^3, d is the measured polymer film thickness in nanometers, and m is the number of functional groups per repeat unit (m = 2, 4, and 1, respectively, for main-chain aromatic, C–O, and other functional groups in Table II). A similar equation was used to obtain the number of bonds broken or formed by chain scission or cross-linking:

$$D_S = [254dC/\bar{M}_n(0)]S \qquad (4)$$

where S is the number of scission or cross-linking events per original polymer chain, and the initial number-average molecular weights $\bar{M}_n(0)$ for I–V are given in Table I. For chain scission, $S = (\bar{M}_n(0)/\bar{M}_n) - 1$,[10,11] and for cross-linking, $S = (\bar{M}_n/\bar{M}_n(0)) - 1$.

The results of the quantum yield calculations applied to the laser-exposed samples of I–V are summarized as a function of the irradiation wavelength in Figures 17–20 and 22–25. In these figures, quantum yields *for bond breaking* or depletion processes, such as chain scission, *are shown on inverted scales* to distinguish them from processes such as cross-linking which involve *bond formation* or accumulation.

Error limits are reported in each figure caption as percentages of the quantum yield values. The error limits associated with the spectroscopic quantum yield measurements were determined from the average signal-to-noise ratios at each fundamental frequency in the subtraction spectra showing changes in type III BPA-PC samples. The error limits were lower for samples showing greater spectral changes upon exposure. For a given sample, the error limits were also lower for stronger absorbers (Table II). The error limits for chain scission or cross-linking were determined from the average precision of measurement of molecular weight *changes* (eq 4). The average precision of the sample molecular weight measurements alone was ±3%. The sample thickness measurements and optical models were not the predominant sources of error.

Quantum yields for depletion of free carbonate carbonyl bonds (1776 cm^{-1}) and C–O bond depletion (1247 and 1235 cm^{-1}) are plotted in Figure 17 and 18, respectively. The quantum yields for carbonyl bond breaking (Figure 17) generally increase with decreasing content of phenolic end groups, although the decrease in UV absorbance with decreasing phenolic end-group content (Figures 4 and 5)
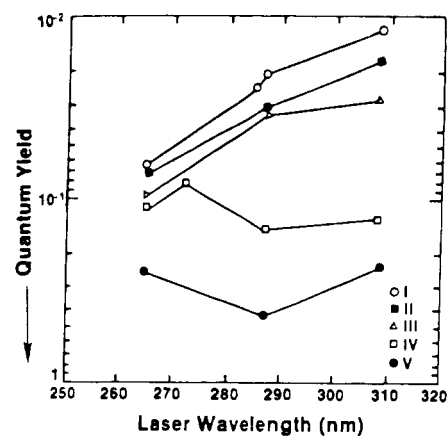

Figure 18. Quantum yields of carbonate C–O bond depletion (1247 cm^{-1}, I–III; 1235 cm^{-1}, IV, V) in BPA-PC at several laser irradiation wavelengths. Error is ±4%.
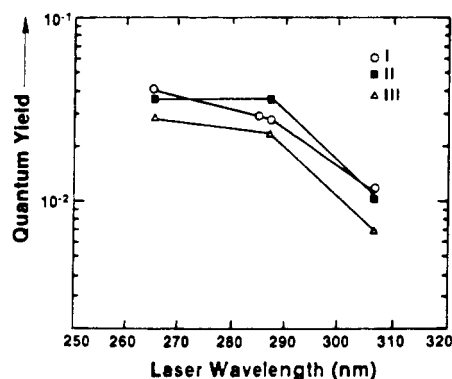

Figure 19. Quantum yields of C–O bond accumulation (1225 cm^{-1}) in BPA-PC (I–III) at several laser irradiation wavelengths. Error is ±4%.

is relatively greater, so that the rate of degradation in mostly capped polymers IV and V is less than in I–III for equivalent irradiance levels. Note the maxima for quantum yields of carbonyl and C–O loss at 287 nm in IV and V. We postulate that the difference in wavelength dependence of photodegradation of these polymers from that of I–III at 287 nm is attributable to a difference in the hydrogen-bonding interactions of the phenolic end groups. In I–III, the phenolic chain ends are predominately hydrogen bonded to main-chain carbonyl groups. Polymers IV and V contain only a small concentration of phenolic end groups, and these groups are apparently not bonded to carbonyl groups but may be bonded to small polar molecules, such as water, in the polymer matrix.[37] The equilibrium concentrations of absorbed water in IV and V at room temperature are expected to exceed the concentration of phenolic end groups in these polymers (Table I) by at least an order of magnitude.[38] Comparison of Figures 17 and 18 reveal the qualitative similarity in the wavelength-dependent quantum yields calculated for degradation of carbonate carbonyl and C–O groups, indicating that most of the photodegradation of carbonyl groups involves the entire carbonate unit. The higher quantum yields for C–O loss relative to carbonate loss arise from the stochiometric factor m = 4 in eq 3.

The quantum yields for C–O *accumulation* determined at 1225 cm^{-1} in I–III are plotted in Figure 19. Smaller increases in the C–O absorption also probably occur at 1225 cm^{-1} in IV and V, although they were not quantified with the optical model. The wavelength dependence of the quantum yields for C–O accumulation at 1225 cm^{-1} differs from that of other processes which involve the
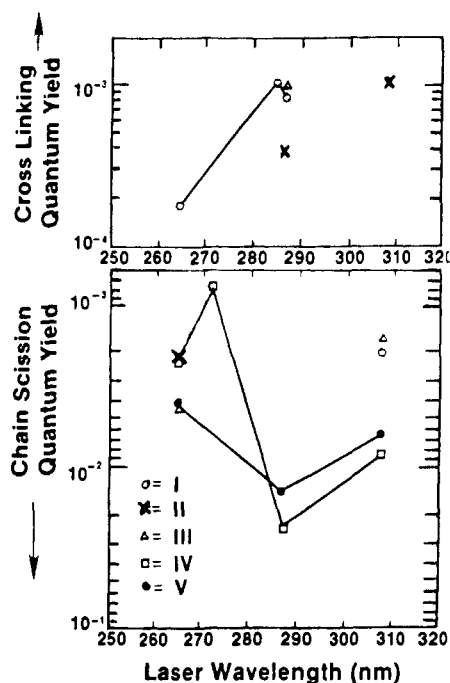
Figure 20. Quantum yields of chain scission or cross-linking in BPA-PC (I–V) at several laser irradiation wavelengths. Error is ±30%.

carbonate or aromatic backbone in that the yields for C–O accumulation are higher at 285–287 nm relative to the other processes. The C–O accumulation process is apparently independent of the other processes and is probably localized on the aliphatic isopropylidene group. Depletion of aliphatic C–H bonds was also noted, although the BPA-PC films were too thin to enable quantitative determination of changes in k_2 for the weak aliphatic C–H absorption at 2940 cm^{-1}, as predicted previously.[24] The increases in C–O absorption at 1225 and 1170 cm^{-1} (Figure 15, not modeled) are consistent with the IR spectrum of *tert*-butyl hydroperoxide.[27] The role of hydroperoxides in the photooxidation of polycarbonates has been postulated by Factor and Chu,[12] and hydroperoxides have been measured by titration[14] and by SO_2 labeling followed by ESCA[39] in exposed BPA-PC. The precursors of the hydroperoxides in I–III are evidently oxygen charge-transfer complexes on the isopropylidene portion of BPA-PC repeating units adjacent to phenolic end groups either on the same or on different BPA-PC molecules. These complexes exhibit a tailing UV absorption at wavelengths as long as 350 nm.[12] The increase in quantum efficiency for

hydroperoxide formation in BPA-PC with decreasing irradiation wavelength (Figure 19) is consistent with an earlier study of the wavelength dependence of photooxidation of BPA-PC by Munro and Allaker.[15] In our study, the quantum yields for this process were generally found to increase with content of phenolic end groups, which is consistent with studies by Pryde[16] on oxidation of BPA-PC containing added BPA. This latter observation also explains the difficulty in observing the band increases at 1225 and 1170 cm^{-1} in IV and V (Figure 13) and the difficulty that other researchers[12] experienced in measuring hydroperoxides in exposed samples of BPA-PC similar to IV, which contain a low initial concentration of phenolic end groups.

The quantum yields (Figure 20) for degradation processes affecting molecular size in I–V calculated from SEC data show a dramatic wavelength dependence. Cross-linking and chain scission reactions apparently occur simultaneously in the exposed samples, as shown by the increase in polydispersity index measured for all samples after exposure, in accordance with a study by Pryde.[16] However, the effect of the hydrogen-bonded phenolic end groups in I–III is to cause a cross-linking reaction to predominate over chain scission at 285–287 nm, within the UV absorption band of the phenolic end groups. The quantum yields of this cross-linking reaction are less than those determined spectroscopically for most of the other degradation processes. It is likely, based on existing literature,[40] that the initial reaction involves selective absorption of 285–287-nm radiation by the terminal phenol, energy transfer to the adjacent hydrogen-bonded carbonyl, and abstraction of the phenolic proton by the excited carbonyl to create a phenyl–carbonate radical pair. Thermal decay of this radical pair would establish a cross-link to the terminal phenyl radical. Abstraction of the ortho hydrogen by the carbonate radical would create an alternate cross-linking site. The proposed mechanistic pathways are sketched in Figure 21, with the polycarbonate main chain in the conformation proposed by Williams and Flory.[41] At 265 and 272 nm, absorption by unbonded carbonyl and main-chain aromatic groups in I–III predominates and the probability of chain scission is increased. Scission is also favored in I and III at 308 nm, but II exhibits anomalous cross-linking (possibly an experimental artifact). In all samples of I–III exhibiting scission, SEC showed accumulation of BPA monomer, dimer, and trimer. In exposed samples of V, the lower molecular weight fragments were not resolved into distinct fractions and were not detected in IV because of the SEC column type used. In IV and V, a high yield of chain
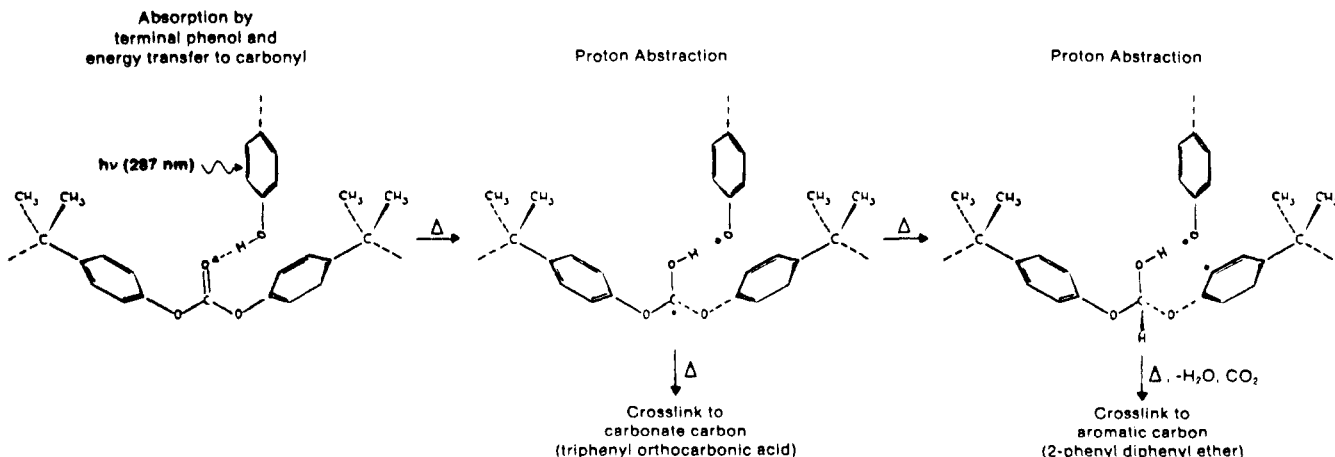

Figure 21. Proposed cross-linking mechanisms involving terminal phenolic groups in BPA-PC.
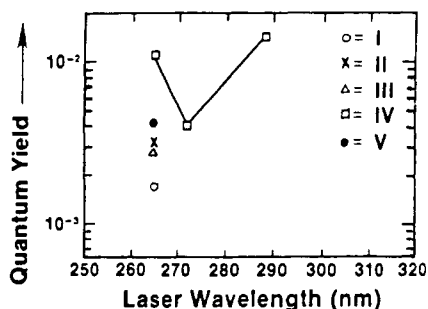
Figure 22. Quantum yields of photo-Fries rearrangement (1685 cm^{-1}) in BPA-PC (I–V) at several laser irradiation wavelengths. Error is ±7%.

scission is observed at 287 nm. The dramatic difference in behavior between I–III and IV and V at 287 nm is apparently attributable to the predominance of terminal phenols which are hydrogen bonded to main-chain carbonyl units in I–III. Terminal phenolic absorption is still detectable in IV and V at 285–287 nm (Figure 6), but the absorbing phenolic end groups are evidently not hydrogen bonded to carbonyl groups. They are, however, capable of initiating a high yield of chain scission. Since the measured yields for scission at wavelengths less than 308 nm in I–V are less than those for carbonyl loss (Figure 17) corrected for photorearrangement, it is likely that scission reactions in I–V at short wavelengths include both random chain scission and an end-scission process, which yields small fragments that are undetectable by SEC because of their size or volatility under the exposure conditions. Volatile products of BPA-PC photodegradation have been identified by Factor and Chu[12] and end scission has been postulated by Pryde[16] to explain similar SEC data for exposed BPA-PC. The end-scission process may be a hydrolysis reaction that is autocatalyzed by terminal phenols.[18] The reactant water could be present initially at the terminal phenols[37] or could be produced by photo-oxidation.[12] That the quantum yield for chain scission is higher in V than in IV at 265 nm and that this order is reversed at 287 and 308 nm are apparently due to the instability of the acetyl end groups in V relative to that of the main-chain carbonyl groups at 265 nm, where both groups absorb strongly. The relative instability of the acetyl end groups may be due to a lower probability of recombination of radical end-group fragments, which may be more mobile in the glassy matrix than radical main-chain fragments.[42]

The wavelength dependence of the quantum yields for photo-Fries rearrangement in I–V is illustrated in Figure 22. These yields probably represent photo-Fries 1 for the most part, since k_2 for photo-Fries 1 (salicylate) at 1685 cm^{-1} is ca. 10 times that of photo-Fries 2 (dihydroxybenzophenone) at 1690 cm^{-1}. Note that no photo-Fries rearrangement is observed in I–V at 308 nm, in accord with earlier studies of BPA-PC irradiated at long wavelengths in oxygen.[14–16,43] Photorearrangement is detectable at 287 nm only in IV; rearrangement in I–III at this wavelength is evidently inhibited by the terminal phenolic units which are hydrogen bonded to carbonyl in I–III. The UV absorbance of V at 287 nm may be low enough to preclude formation of a detectable concentration of rearrangement products. At 265 nm, rearrangement was observed in all polymers studied. In V, a carbonyl absorbance increase at 1644 cm^{-1}, indicative of Fries-like rearrangement of the acetyl end groups in V, was also observed. This process evidently competes with photo-Fries rearrangement of main-chain carbonate groups, since yields for the latter process are significantly higher at 265 nm in IV than V.
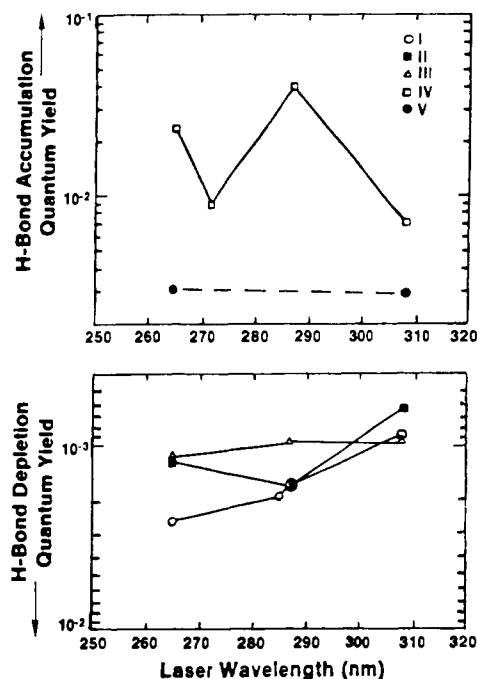

Figure 23. Quantum yields of hydrogen-bonded carbonyl accumulation or depletion (1750 cm^{-1}) in BPA-PC (I–V) at several laser irradiation wavelengths. Error is ±18%.

The quantum yield measured for rearrangement from IR-RA spectral changes in a sample of IV (Figure 11) irradiated with broad-band UV ($\lambda > 260$ nm) was 1.05×10^{-2}, close to the yields measured with laser radiation at 265 and 287 nm (Figure 22) and reasonably close to the yield of 3.5×10^{-2} measured for photo-Fries 1 in solid BPA-PC under continuous irradiation at 254 nm by Gupta and Liang[34] and by Rivaton et al.[14] These data provide a further indication that photodegradation processes induced by controlled exposure to pulsed laser radiation in these samples do not differ dramatically from those that would be induced by continuous exposure to monochromatic light of the same wavelength and that exposure to polychromatic radiation induces different processes which occur simultaneously. The data in Figure 22 show significant wavelength dependence over an interval of only 7 nm.

In contrast to main-chain carbonyl (1776 cm^{-1}), which is depleted in I–V at all laser irradiation wavelengths, hydrogen-bonded carbonyl (1750 cm^{-1}) accumulates in IV at all irradiation wavelengths and in V at 265 and 308 nm. These results indicate that more polar groups were accumulated than were depleted during irradiation of IV and V. The quantum yields for accumulation of hydrogen-bonded carbonyl (Figure 23) are lower in V at these wavelengths than in IV, and no hydrogen-bonded carbonyl was detected in V following irradiation at 287 nm. In I–III, hydrogen-bonded carbonyl groups associated with terminal phenols were depleted at all wavelengths. At 285 and 287 nm, the quantum yields for depletion of hydrogen-bonded carbonyl in I–III are roughly equal to those for cross-linking (Figure 20), indicating that cross-linking in these polymers is initiated at the hydrogen-bonded carbonyl groups.

Resolution of the IR-RA data was sufficient to enable independent determination of the changes in concentration induced in the main-chain aromatic (1507 cm^{-1}) and terminal phenolic (1515 cm^{-1}) groups of I–V by laser irradiation. The quantum yields for depletion or accumulation of these groups are plotted as a function of laser irradiation wavelength in Figures 24 and 25, respectively. These yields are calculated for single aromatic rings rather than repeat
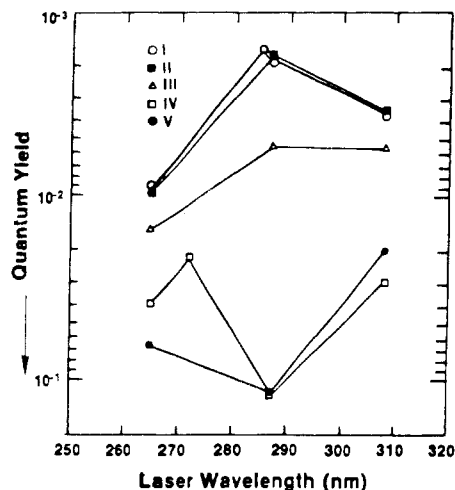
Figure 24. Quantum yields of main-chain aromatic depletion (1507 cm^{-1}) in BPA-PC (I–V) at several laser irradiation wavelengths. Error is ±12%.
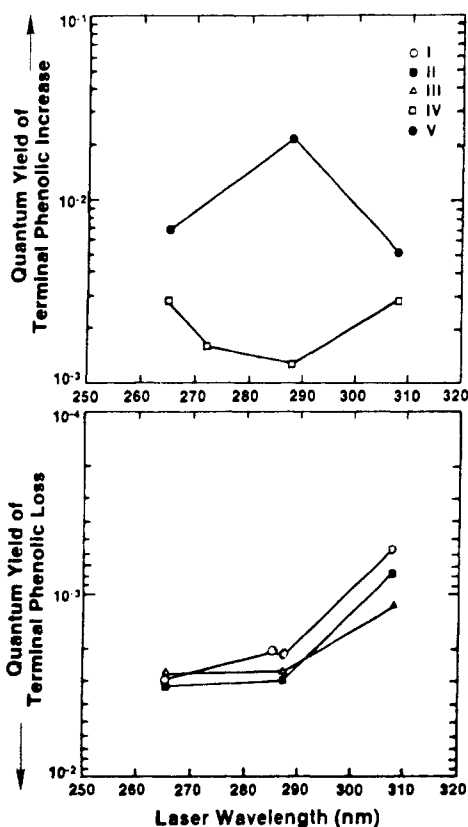

Figure 25. Quantum yields of terminal phenolic depletion or accumulation (1515 cm^{-1}) in BPA-PC (I–V) at several laser irradiation wavelengths. Error is ±6%.
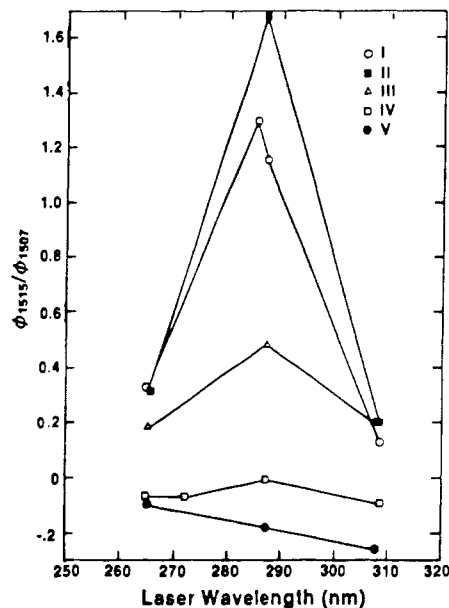

Figure 26. Ratio of quantum yields of terminal phenolic depletion or accumulation (1515 cm^{-1}) to quantum yields of main-chain aromatic depletion (1507 cm^{-1}) at several laser irradiation wavelengths.

units; i.e., $m = 2$ in eq 3. The quantum yields for terminal phenolic groups also include depletion or accumulation of BPA monomer, which also exhibits a k_2 maximum at 1515 cm^{-1}. The quantum yields calculated for depletion of main-chain aromatic groups (1507 cm^{-1}) could have been influenced to some extent by accumulation of phenol (1500 cm^{-1}, not modeled), which has been identified[12] as a photodegradation product in BPA-PC.

The sums of quantum yields for main-chain aromatic depletion (1507 cm^{-1}, Figure 24) and terminal phenolic depletion/accumulation (1515 cm^{-1}, Figure 25) are roughly equal to the sums of quantum yields calculated for free carbonyl depletion (1776 cm^{-1}) and hydrogen-bonded carbonyl depletion or accumulation (1750 cm^{-1}) except at

308 nm in I–III, indicating that there is a one-to-one correspondence between aromatic degradation and carbonyl degradation. This observation is consistent with the photo-Fries 1, cross-linking, and chain-scission reaction mechanisms and also indicates that initial photooxidation of the ispropylidene groups in I–III (Figure 19) does not affect the aromatic or carbonate groups, although photooxidation is evidently catalyzed by the terminal phenolic groups in these polymers. The anomaly at 308 nm in I–III is evidently caused by depletion of free and hydrogen-bonded carbonyl groups without concurrent depletion of terminal phenolic groups; in this case, the yields for main-chain aromatic depletion (1507 cm^{-1}) roughly equal the sum of yields for free and hydrogen-bonded carbonyl depletion. Also, the yields of terminal phenol (1515 cm^{-1}) in IV and V (Figure 25) approximate those for chain scission (Figure 20) except at 287 and 308 nm in IV. At these wavelengths, end scission to produce phenol (1500 cm^{-1}) is evidently initiated at the phenolic caps in IV. These observations are consistent with the conclusion of Factor and Chu[12] that chain scission occurs at the carbonate linkages and produces phenolic fragments with unit efficiency. Another likely product of chain scission is CO_2,[20] although CO_2 produced by photooxidation of BPA-PC is expected to predominate by factors of at least 10^2 in the reaction products.[12] This would be true even for experiments done in inert atmospheres unless extraordinary precautions, such as in-situ vacuum melt annealing, were taken to destroy the oxygen–isopropylidene charge-transfer complexes initially present[12] in the samples.

The quantum yield ratios, ϕ_{1515}/ϕ_{1507}, for depletion or accumulation of terminal phenolic groups (1515 cm^{-1}) relative to depletion of main-chain aromatic groups (1507 cm^{-1}) are plotted as a function of laser irradiation wavelength in Figure 26. These plots show positive maxima for depletion of terminal phenolic groups relative to depletion of main-chain aromatic groups in I–III at 285–287 nm. At 265 and 308 nm, the quantum yield ratios ϕ_{1515}/ϕ_{1507} approach (but are greater than) $F/10^2 n$ (Table I), where F is the percentage of phenolic chain ends. This limiting value represents completely random photodegradation based on the initial relative concentrations of these
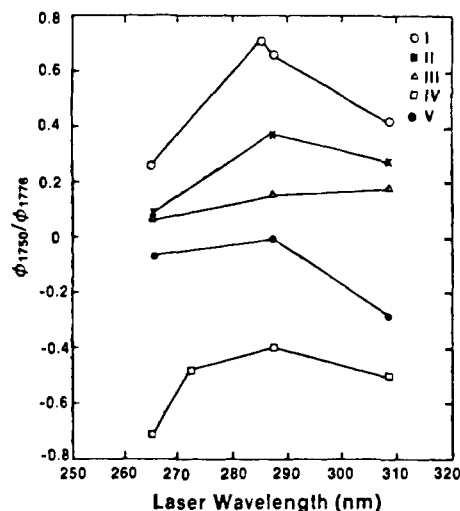
Figure 27. Ratio of quantum yields of hydrogen-bonded carbonyl depletion or accumulation (1750 cm^{-1}) to quantum yields of free carbonyl depletion (1776 cm^{-1}) at several laser irradiation wavelengths.

groups. The relatively low negative ratio of quantum yields for terminal phenolic/aromatic groups in IV at 287 nm suggests that the aromatic degradation processes produce little BPA or terminal phenol. The relatively high quantum yields for most degradation processes in IV at 287 nm (Figures 17, 18, 20, and 22–25) suggest that these processes are catalytically initiated by phenolic end groups in IV which are bonded to water molecules rather than to carbonyl groups. That this does not occur in acetyl-capped V suggests that the primary energy transfer step in IV is from these water-bonded terminal phenols to phenyl caps (Table I) in the polar zones[16] containing end groups in the polymer matrix. That more terminal phenolic groups (or BPA molecules) are produced per main-chain aromatic group destroyed in V than in IV is also consistent with SEC detection of BPA monomer, dimer, and trimer, as well as other low molecular weight fragments, in exposed samples of V. These fragments are probably a result of degradation processes initiated at the acetyl end groups in V, although it should be remembered that the overall photodegradation rate of V is lower than that of IV at 287 and 308 nm because of its lower UV absorbance (Figure 5) at these wavelengths.

The quantum yield ratios for depletion or accumulation of hydrogen-bonded carbonyl groups (1750 cm^{-1}) relative to depletion of free carbonyl groups (1776 cm^{-1}) are plotted in Figure 27. The yield ratios for I–III exceed $F/10^2 n$ at all wavelengths, indicating that hydrogen-bonded carbonyl groups are selectively degraded. Positive maxima for depletion of hydrogen-bonded carbonyl groups relative to free carbonyl groups occur in the plots for I and II at 285–287 nm. Although these maxima are less distinct than those for ϕ_{1515}/ϕ_{1507} (Figure 26), the influence of the phenolic end groups on the carbonyl groups to which they are hydrogen bonded is evident. The relative quantum yield plot for III in Figure 27 shows no maximum at 287 nm, and the quantum yield ratio ϕ_{1750}/ϕ_{1776} for I–III is higher at 308 nm than at 265 nm. These observations indicate that at 285–287 nm, degradation processes of the terminal phenolic groups which do not involve attack on the hydrogen-bonded carbonyl groups predominate. That this attack proceeds with less than unit efficiency can be confirmed by noting that the quantum yields for cross-linking in I–III at 285–287 nm (Figure 20) are less by a factor of 2–3 than the corresponding quantum yields for depletion of terminal phenolic groups (Figure 25), although the

cross-linking yields at 285–287 nm are roughly equal to the corresponding yields for depletion of hydrogen-bonded carbonyl (Figure 23).

In contrast to the yield ratios ϕ_{1515}/ϕ_{1507} (Figure 26), the yield ratios ϕ_{1750}/ϕ_{1776} for IV are more negative than for V. This indicates that degradative accumulation of BPA or terminal phenolic groups does not contribute to a large extent to accumulation of hydrogen-bonded carbonyl groups in IV. The negative yield ratio of IV at 308 nm also precludes involvement by photo-Fries 1, which was not produced at this wavelength, in hydrogen bonding to carbonyl groups in IV. Accumulation of small polar molecules such as water or phenol could account for accumulation of hydrogen-bonded carbonyl in IV. The low negative yield ratios ϕ_{1750}/ϕ_{1776} for V (Figure 27) and the presence of phenyl end groups in IV (Table I) indicate that the hydrogen-bonded carbonyl groups produced by irradiation of IV are associated with photolytically produced phenol. Phenol has a much lower absorption coefficient than BPA at 287 nm (in THF) and would therefore not be expected to contribute to accelerated degradation of the adjacent carbonyl groups at this wavelength as does BPA.[16] The primary photoreaction sequence in IV at 287 nm (aside from photooxidation) is evidently cleavage of the phenyl end groups after catalytic photoinitiation by adjacent phenolic end groups, which predominate in absorbance at this wavelength, followed by end scission of the BPA-PC chain beginning at the cleavage site.
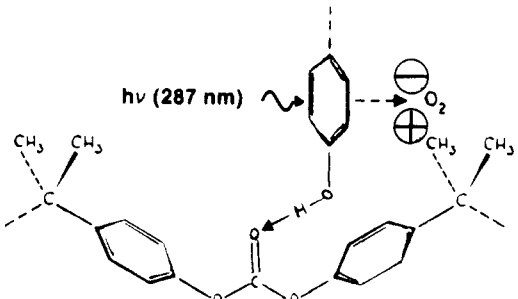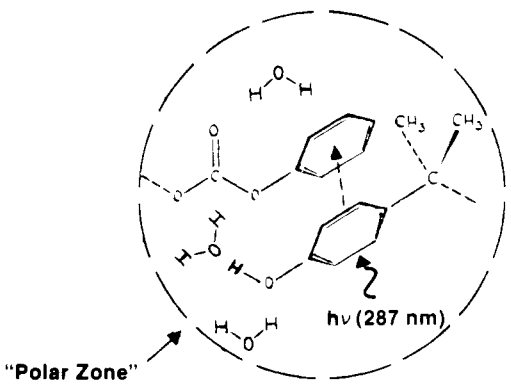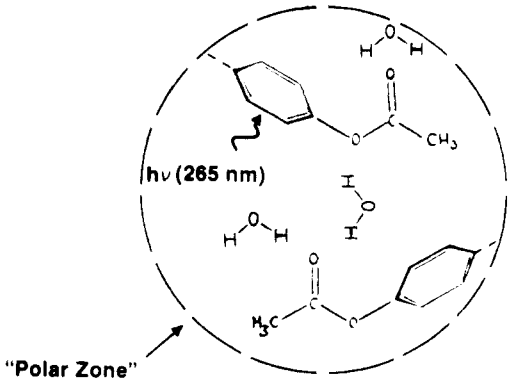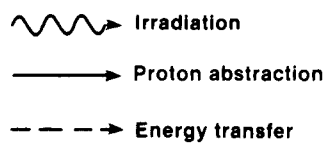
Concluding Remarks

The data obtained in this study are consistent with a number of conclusions (summarized in Table III) regarding the influence of various end groups on the wavelength dependence of photodegradation in BPA-PC. These conclusions are as follows:

1. The differences in the wavelength-dependent photodegradation of I–III from that of IV and V, which are especially obvious at 287 nm, result from differences in hydrogen bonding of the terminal phenolic groups in these polymers. In I–III, the terminal phenols are predominantly hydrogen bonded to carbonyl backbone units, and a significant fraction of these bonds are intermolecular, as evidenced by the cross-linking observed in I–III at 287 nm. Establishment of the hydrogen bonds is a thermally activated process. In IV and V, terminal phenolic groups are present in smaller concentrations than sorbed water and are not hydrogen bonded to carbonyl groups. Competitive hydrogen bonding of water to the terminal phenolic groups in IV and V and the resulting change of these groups from photoreactants (in I–III) to photoinitiators (in IV and V) are postulated to explain the different photodegradation mechanisms observed in these two polymer types, e.g., cross-linking in I–III vs. random chain scission and end scission in IV and V at 287 nm.

2. The quantum yields for accumulation of C–O bonds on the isopropylidene groups in I–III are higher than those calculated for carbonyl depletion. These C–O bonds have been tentatively assigned to hydroperoxide groups on the methyl side groups in BPA-PC. Formation of an oxygen charge-transfer complex on the methyl side groups in BPA-PC evidently precedes photochemical production of hydroperoxides. The observation that quantum yields for hydroperoxide formation generally increase with increasing concentration of terminal phenolic groups in III, II, and I, while quantum yields for free carbonyl degradation decrease in this order, indicates that the terminal phenolic groups in these polymers can act as initiators for photooxidation as well as photoreactants. Either inter- or intramolecular initiation of photooxidation by terminal

Table III
Mechanistic Inferences from Quantum Yield Data

Primary End Group — Matrix Interaction	Primary Photoreactions Observed

I, II, III

hν / 265 nm → Photo-oxidation, carbonate rearrangement, random chain scission, end-scission (to yield BPA)

hν / 287 nm → Photo-oxidation (sensitized by terminal phenol), photolysis of terminal phenol, competing with proton abstraction by carbonyl from terminal phenol followed by crosslinking

hν / 308 nm → Photo-oxidation, random chain scission

IV

"Polar Zone"

hν / 265 nm → Carbonate rearrangement, end-scission, random chain scission

hν / 287 nm → End-scission sensitized by terminal phenol (to yield free phenol), carbonate rearrangement, random chain scission

hν / 308 nm → Random chain scission

V

"Polar Zone"

hν / 265 nm → End-scission (to yield BPA), random chain scission, carbonate rearrangement, acetyl rearrangement

hν / 287 nm → End-scission sensitized by terminal phenol (to yield BPA), random chain scission

hν / 308 nm → Random chain scission

∿∿∿➤ Irradiation

———➤ Proton abstraction

– – – ➤ Energy transfer

phenolic groups is possible. The Dexter,[40] or exchange, mechanism is probably operating in either case, since the Williams–Flory model for BPA-PC conformation[41] would accommodate close proximity of a terminal phenol hydrogen bonded to carbonyl and the methyl side chains in a BPA-PC molecule. Also, there is considerable overlap between the UV absorption spectrum[12] of the oxygen charge-transfer complex and the UV emission spectrum of BPA for 282-nm excitation[44] (and, by inference, the emission spectrum for 287-nm excitation of terminal phenolic groups in I–III), so that the exchange overlap integral[40] is nonzero. Photophysical techniques such as

fluorescence lifetime measurements and quenching rate studies of I–III for 287-nm excitation would be helpful in verifying this hypothesis.

3. Terminal phenolic chain ends in I–III are depleted preferentially to main-chain aromatic groups, especially at 287 nm. Hydrogen-bonded carbonyl in these polymers is also depleted preferentially to main-chain carbonyl at 287 nm, although the quantum yield ratio for the latter processes is less than the phenolic/aromatic yield ratios. This indicates that some of the terminal phenolic groups underwent photolysis at 287 nm without undergoing cross-linking or other reactions with the carbonyl groups

to which they were hydrogen bonded. In IV and V, both terminal phenolic groups and hydrogen-bonded carbonyl groups are formed during exposure rather than being depleted as in I–III. Terminal phenol and BPA are formed to a greater extent in V than in IV. In IV, formation of phenol, possibly resulting from photolysis of the phenyl end groups, evidently predominates.

4. Photo-Fries rearrangement is not observed at 308 nm. It is observed at 287 nm only in IV; photo-Fries rearrangement is observed in all polymers studied at 265 nm, with quantum yields increasing in the order I < III < II < V < IV. These observations indicate that the terminal phenolic groups hydrogen bonded to carbonyl in I–III inhibit this reaction and that terminal phenolic groups not bonded to carbonyl in IV catalyze it. In V, Fries rearrangement of acetyl chain ends competes with backbone carbonate rearrangement at 265 nm. Quantum yields for photo-Fries rearrangement in laser-irradiated samples and samples exposed to broad-band UV radiation over similar wavelength ranges are comparable, indicating that nonlinear photochemistry was not a factor in the degradation of the laser-exposed samples.

Registry No. (BPA)(PC) (SRU), 24936-68-3; (BPA)(PC) (copolymer), 25037-45-0; IPDA, 10192-62-8; V, 104335-97-9.

References and Notes

(1) Schissel, P.; Czanderna, A. W. *Solar Energy Mater.* **1981**, *3*, 225.
(2) Blaga, A.; Yamasaki, R. S. *J. Mater. Sci.* **1976**, *11*, 1513.
(3) Davis, A.; Golden, J. H. *J. Macromol. Sci., Rev. Macromol. Chem.* **1969**, *C3*(1), 49.
(4) Ram, A.; Zilber, O.; Kenig, S. *Polym. Eng. Sci.* **1981**, *25*, 535.
(5) Huyett, R. A.; Wintermute, G. E. *Air Force Mater. Lab., Tech. Rep. AFML-TR (U.S.)* **1976**, *AFML-TR 76-24*, 129.
(6) Klein, W. H.; Goldberg, B. In *Sun: Proceedings, ISES*; Winter, F., Cox, M., Eds.; Pergamon: New York, 1978; pp 400–414.
(7) Zerlaut, G. A. In *Proceedings, American Gas Association Operating Section*; American Gas Association: Arlington, VA, 1984; pp 12–19.
(8) Barker, R. E. *Photochem. Photobiol.* **1968**, *7*, 275.
(9) Bellus, D.; Hrdlovik, P.; Manasek, Z. *J. Polym. Sci., Part B* **1966**, *4*, 1.
(10) Humphrey, J. S.; Schultz, A. R.; Jaquiss, D. B. G. *Macromolecules* **1973**, *6*, 305.
(11) Gupta, A.; Renbaum, A.; Moacanin, J. *Macromolecules* **1978**, *11*, 1285.
(12) Factor, A.; Chu, M. L. *Polym. Degrad. Stab.* **1980**, *2*, 203.
(13) Clark, D. T.; Munro, H. S. *Polym. Degrad. Stab.* **1984**, *8*, 195.
(14) Rivaton, A.; Sallet, D.; Lemaire, J. *Polym. Photochem.* **1983**, *3*, 463.
(15) Munro, H. S.; Allaker, R. S. *Polym. Degrad. Stab.* **1985**, *11*, 349.
(16) Pryde, C. A. *ACS Symp. Ser.* **1985**, *No. 280*, Chapter 23.
(17) Adam, G. A.; Hay, J. N.; Parsons, I. W.; Haward, R. N. *Polymer* **1976**, *17*, 51.
(18) Pryde, C. A. *J. Appl. Polym. Sci.* **1980**, *25*, 2573.
(19) Webb, J. D.; Schissel, P.; Czanderna, A. W.; Chughtai, A. R.; Smith, D. M. *Appl. Spectrosc.* **1981**, *35*, 598.
(20) Webb, J. D.; Schissel, P.; Thomas, T. M.; Pitts, J. R.; Czanderna, A. W. *Solar Energy Mater.* **1984**, *11*, 163.
(21) Merrill, S. H. *J. Polym. Sci.* **1961**, *55*, 343.
(22) Yau, W. W.; Kirkland, J. J.; Bly, D. D. *Modern Size-Exclusion Chromatography*; Wiley: New York, 1979; p 8.
(23) Webb, J. D. *Solar Energy Res. Inst. Techn. Rep. 255-2177* **1984**, *1*.
(24) Webb, J. D.; Jorgensen, G.; Schissel, P.; Czanderna, A. W.; Chughtai, A. R.; Smith, D. M. *ACS Symp. Ser.* **1983**, *No. 220*, Chapter 9.
(25) Factor, A. Personal communication, 1985.
(26) Ordal, M. A. *Appl. Opt.* **1983**, *22*, 1099.
(27) Pouchert, C. J., Ed. *Aldrich Library of Infrared Spectra*; Aldrich Chemical Co.: Milwaukee, WI, 1978; p 762.
(28) Varnell, D. F.; Runt, J. P.; Coleman, M. M. *Macromolecules* **1981**, *14*, 1350.
(29) Allara, D. L.; Baca, A.; Pryde, C. A. *Macromolecules* **1978**, *11*, 1215.
(30) Farenholtz, S. R. *Macromolecules* **1982**, *15*, 937.
(31) Ribbegard, G. K.; Jones, R. N. *Appl. Spectrosc.* **1980**, *34*, 638.
(32) Graf, R. T.; Koenig, J. L.; Ishida, H. *Appl. Spectrosc.* **1985**, *39*, 405.
(33) Van Scoy, R. L. *Photonics Spectra* **1985**, *19*, 53.
(34) Gupta, A.; Liang, R. *Macromolecules* **1980**, *13*, 262.
(35) Johnson, P. B.; Christy, R. W. *Phys. Rev. B.* **1972**, *6*, 4370.
(36) Bohn, L. In *Polymer Handbook*; Brandrup, J., Immergut, E. H., Eds.; Wiley: New York, 1975; p III-243.
(37) Rivaton, A.; Sallet, D.; Lemaire, J. *Polym. Degrad. Stab.* **1986**, *14*, 23.
(38) Suzuki, T. H.; Chirara, H.; Kotaka, T. *Polym. J.* **1984**, *16*, 129.
(39) Clark, D. T.; Munro, H. S. *Polym. Degrad. Stab.* **1982**, *4*, 441.
(40) Turro, N. J. *Modern Molecular Photochemistry*; Benjamin-Cummings: Menlo Park, CA, 1978; pp 362–413.
(41) Williams, A. D.; Flory, P. J. *J. Polym. Sci., Part A2* **1968**, *6*, 1945.
(42) Moore, J. W. Thesis, University of Toronto, 1983.
(43) Rivaton, A.; Sallet, D.; Lemaire, J. *Polym. Degrad. Stab.* **1986**, *14*, 1.
(44) *Sadtler Fluorescence Spectral Library*; Sadtler Research Laboratories: Philadelphia, PA, 1976; No. 1011.